SIAM J. SCI. COMPUT.
Vol. 30, No. 1, pp. 525–547

SAMPLING ROTATION GROUPS BY SUCCESSIVE ORTHOGONAL IMAGES*

JULIE C. MITCHELL†

Abstract. The ability to construct uniform deterministic samples of rotation groups is useful in many contexts, but there are inherent mathematical difficulties that prevent an exact solution. Here, we present successive orthogonal images, an effective means for uniform deterministic sampling of orthogonal groups. The method is valid in any dimension, and analytical bounds are provided on the sampling uniformity. Numerical comparisons with other sampling methods are given for the special case of $\mathbf{SO}(3)$. We make use of non-Riemannian distance metrics that are group-invariant and locally compatible with the Haar measure. In addition, our results provide a semi-unique decomposition of any orthogonal matrix into the product of planar rotations.

Key words. orthogonal group, dispersion, uniform sampling, Haar measure, $\mathbf{SO}(3)$, $\mathbf{SO}(n)$

AMS subject classifications. 31B99, 31C12, 52C17, 51F25, 52C22, 65D99, 81U10, 81U30

DOI. 10.1137/030601879

1. Background and introduction.

The orthogonal and unitary groups have important applications in structural biology [7, 8, 17, 19, 31], computation [4, 5, 15, 27], motion planning [12, 33], and cryptography [10], to name but a few. In addition, deterministic uniform sampling on spheres and other spaces is an important and long-studied problem in mathematics and statistics [13, 16, 18, 24, 26].

Here, we present successive orthogonal images (SOI), an approach to uniform deterministic sampling of the rotation group in n dimensions, $\mathbf{SO}(n)$. The construction was previously described for the three-dimensional rotation group and applied to the prediction of protein binding geometry [19]. The results of this manuscript refine the sampling method and extend it to higher dimensions. A nontechnical overview given in the next section may be most useful to application scientists, along with codes that may be obtained from the author's website.

Our goal is to construct deterministic samples that cover $\mathbf{SO}(n)$ at an approximate length step, in a well-dispersed fashion. For our own application of interest, molecular docking, this offers a couple of advantages. First, we use a minimal number of points to guarantee sampling at some level of resolution. Because docking calculations are expensive (at least with present technology), this efficiency is desirable. Also, uniformly distributing the sample points makes integral approximations, such as the Boltzmann weighted average [19], possible via simple summation.

The paper proceeds with a brief introduction to $\mathbf{SO}(n)$ and its Haar measure. We then use the Froebenius norm to define a projective Euclidean distance metric on $\mathbf{SO}(n)$, using a natural duality with the Riemannian distance metric. The ability to distribute points (locally) relative to the Haar measure is unaffected by the use of a non-Riemannian distance metric, because the distance function is invariant under the action of the group and closely approximates the Riemannian distance metric.

*Received by the editors November 18, 2003; accepted for publication (in revised form) August 27, 2007; published electronically February 8, 2008. This project was supported in part by the U.S. Department of Energy awards DE-FG03-01ER25497 and DE-FG02-04ER25627 and a fellowship from the Alfred P. Sloan Foundation.

http://www.siam.org/journals/sisc/30-1/60187.html

†Departments of Mathematics and Biochemistry, University of Wisconsin-Madison, 480 Lincoln Dr., Madison, WI 53706 (mitchell@math.wisc.edu).

Next, we discuss uniform deterministic sampling on $\mathbf{SO}(3)$ as a special case. SOI will be compared with two other approaches, the layered Sukharev [33] and variable stepping [31] methods. The three methods are analyzed numerically using a variety of uniformity criteria. In each case, SOI outperforms the other two methods, particularly in achieving near-optimal nearest neighbor spacing. Finally, for the general case of $\mathbf{SO}(n)$, analytical results are derived for the global coverage and local separation of SOI samples. Global coverage and local separation are related, but not identical, to existing notions of dispersion and discrepancy. Dispersion is designed for the case when one wants to distribute a fixed number of points in an optimally uniform fashion, whereas we attempt to solve the converse problem of sampling the rotation group uniformly at some length step.

The paper develops a matrix decomposition that expresses any transformation in $\mathbf{SO}(n)$ as a sequence of simple planar rotations that are similar to, but distinct from, Givens transformations [14]. This allows certain machinery available for $\mathbf{SO}(3)$ to be applied in the context of $\mathbf{SO}(n)$. The decomposition has been used in a natural way to prove a theorem establishing the global coverage (i.e., dispersion) qualities of SOI samples. The matrix decomposition may be of use in numerical linear algebra, though we explore it in relation to uniform rotational sampling. In our case, the decomposition is key to constructing uniform samples on $\mathbf{SO}(n)$ from uniform samples of the i-dimensional spheres $\mathbf{S}^i$ for $i < n$.

1.1. A nontechnical overview. Much of the paper is devoted to establishing uniformity results for SOI samples of the rotation groups. However, given the many applications of orthogonal groups, we begin with an accessible introduction for the nonspecialist. Our objective is to uniformly sample the rotation group at some approximate length step. A rotation group has curvature, like that of a sphere. This and other properties make it impossible to sample the space using a perfect lattice. Here, though, we demonstrate that it is possible to generate deterministic samples that are lattice-like in some respects.

In three dimensions, we can specify a rotation, $\mathbf{M}$, using three mutually orthogonal vectors $\{\mathbf{u}_0, \mathbf{u}_1, \mathbf{u}_2\}$. These are the images (under $\mathbf{M}$) of the principal unit vectors $\mathbf{x}_0 = (1, 0, 0), \mathbf{x}_1 = (0, 1, 0)$, and $\mathbf{x}_2 = (0, 0, 1)$. Our method uses a spherical sample, $\mathbf{U}^2$, to define the possible choices of $\mathbf{u}_2$, as in Figure 1.1. Given a specific $\mathbf{u}_2$, the remaining vectors must be orthogonal to it. Then $\mathbf{u}_1$ is constrained to a ring in the plane orthogonal to $\mathbf{u}_2$. A sample, $\mathbf{U}^1$, on this ring determines the possible choices of $\mathbf{u}_1$. Once $\mathbf{u}_1$ and $\mathbf{u}_2$ are chosen, $\mathbf{u}_0$ is determined by the orthogonality constraints. A sample, $\mathbf{U}$, of the rotation space consists of all possible combinations of $\{\mathbf{u}_0, \mathbf{u}_1, \mathbf{u}_2\}$, varied over a uniform sample of a sphere and uniform samples of the orthogonal rings. To build a globally uniform sample of the rotation group, it is important that the sampling rates are balanced correctly.

For rotations in four-dimensional space, we start by sampling a three-dimensional sphere, repeating the process for two- and one-dimensional spheres. Each new dimension brings an added level of sampling on a higher dimensional sphere. This is mathematically sound and almost fantastically simple, but establishing the uniformity of deterministic samples generated in this way requires some care. To obtain these results, we will make use of norms that are common to numerical analysis and apply them in the context of geometry. In a sense, these norms provide a local Euclidean approximation to the angular distance measures on these curved spaces, from which a Pythagorean-like theorem results.

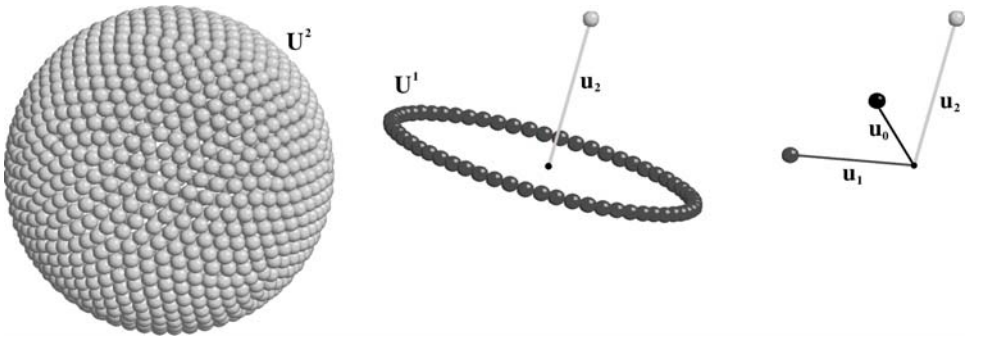

FIG. 1.1. *Uniform deterministic sampling of* $\mathbf{SO}(3)$. *The figure shows a uniformly distributed set,* $\mathbf{U}^2$, *of possible choices for* $\mathbf{u}_2 = \mathbf{M}\mathbf{x}_2$. *Center: Once a choice of* $\mathbf{u}_2$ *is made,* $\mathbf{u}_1 = \mathbf{M}\mathbf{x}_1$ *is chosen from a uniform sample,* $\mathbf{U}^1$, *of the subspace orthogonal to* $\mathbf{u}_2$. *Once* $\mathbf{u}_1$ *and* $\mathbf{u}_2$ *are chosen,* $\mathbf{u}_0$ *is determined from the orthogonality constraints. The key to achieving global sampling uniformity is to balance the number of sample points in each subspace. This method generalizes to higher dimensional* $\mathbf{SO}(n)$ *by recursive sampling, starting from higher dimensional spheres.*

1.2. The special orthogonal group, $\mathbf{SO}(n)$. The *orthogonal group*, $\mathbf{O}(n)$, is the set of all $n \times n$ matrices for which $\mathbf{M}^t = \mathbf{M}^{-1}$. Orthogonal matrices must have mutually orthogonal row/column vectors and $\det(\mathbf{M}) = \pm 1$. The eigenvalues, $\boldsymbol{\xi}_i$, of $\mathbf{M} \in \mathbf{O}(n)$ are real or complex numbers satisfying $|\boldsymbol{\xi}_i| = 1$ for $i = 0, \ldots, n-1$.

We are mainly concerned with the *special orthogonal group,* $\mathbf{SO}(n)$, of orientation-preserving elements of $\mathbf{O}(n)$, although all of the sampling results carry over to $\mathbf{O}(n)$ in a natural way. The space $\mathbf{SO}(n)$ consists of those elements of $\mathbf{O}(n)$ for which $\det(\mathbf{M}) = 1$. An element of $\mathbf{SO}(n)$ can be viewed as an isometric, orientation-preserving change of coordinates on $\mathbb{R}^n$, and properties that are invariant under an orthonormal change of basis are naturally preserved by the group action of $\mathbf{SO}(n)$.

Throughout, we will denote by $\mathbf{x}_i$ the ith principal unit vector in $\mathbb{R}^n$, with numbering from $i = 0$ chosen for later convenience of notation. When working with an element $\mathbf{M} \in \mathbf{SO}(n)$, we will denote by $\mathbf{M}\mathbf{x}_i$ the image under $\mathbf{M}$ of the vector $\mathbf{x}_i$. The coordinates of $\mathbf{M}\mathbf{x}_i$ are taken from the ith column of $\mathbf{M}$, which we generally regard as a matrix relative to an orthonormal basis $\{\mathbf{x}_0, \ldots, \mathbf{x}_{n-1}\}$ of $\mathbb{R}^n$.

For any set of $(n-1)$ mutually orthogonal unit vectors $\{\mathbf{u}_i = \mathbf{M}\mathbf{x}_i : \mathrm{i} = 1, \ldots, (n-1)\}$ in $\mathbb{R}^n$, there is a unique choice of $\mathbf{u}_0 = \mathbf{M}\mathbf{x}_0$ such that $\mathbf{M} \in \mathbf{SO}(n)$. This can be thought of as a generalization of the cross product, and in fact it is possible to write the $\mathbf{u}_i$ as rows in a matrix and define the coordinates of $\mathbf{u}_0$ as determinants of the $(n-1) \times (n-1)$ submatrices, following the example of the cross product for $n = 3$. The product of $\mathbf{u}_1 \times \mathbf{u}_2 \times \cdots \times \mathbf{u}_{n-1}$ defines the vector $\mathbf{u}_0$, and it is easy to see that

$$\begin{aligned} \det(\mathbf{M}) &= \langle \mathbf{u}_0, \mathbf{u}_1 \times \mathbf{u}_2 \times \cdots \times \mathbf{u}_{n-1} \rangle \\ &= \langle \mathbf{u}_0, \mathbf{u}_0 \rangle \\ &= 1. \end{aligned}$$

1.3. Haar measure and uniform sampling. $\mathbf{SO}(n)$ is a *Lie group*. This means it is both a group and a manifold, and its group actions are diffeomorphisms. Each element $\mathbf{M} \in \mathbf{SO}(n)$ defines a left (right) group action given by $\mathbf{N} \to \mathbf{M} \cdot \mathbf{N}$ $(\mathbf{N} \to \mathbf{N} \cdot \mathbf{M})$. Up to a scalar multiple, there exists a unique measure on $\mathbf{SO}(n)$ that is invariant with respect to group actions. This is called the *Haar measure*. The Haar measure is the one for which all group actions are global isometries. In our

particular situation, we can think of the Haar measure as being invariant under all orthogonal coordinate changes.

A scheme for randomly choosing an element of $\mathbf{M} \in \mathbf{SO}(n)$ is uniform with respect to a measure $\boldsymbol{\mu}$ if, for any measurable subsets $\boldsymbol{\Omega}_1, \boldsymbol{\Omega}_2 \subset \mathbf{SO}(n)$, one has

$$\boldsymbol{\mu}(\boldsymbol{\Omega}_1) = \boldsymbol{\mu}(\boldsymbol{\Omega}_2) \qquad \Longleftrightarrow \qquad P(\mathbf{M} \in \boldsymbol{\Omega}_1) = P(\mathbf{M} \in \boldsymbol{\Omega}_2). \tag{1.1}$$

In other words, $\mathbf{M}$ has equal probability of being chosen from $\boldsymbol{\Omega}_1$ or $\boldsymbol{\Omega}_2$ precisely when they have the same measure. In fact, by normalizing $\boldsymbol{\mu}$ so that the entire space has unit volume, one retrieves the uniform probability measure. For deterministic sampling, there is no absolute agreement on how to best measure deviation from uniformity. We will return to this issue in section 2.3 and provide numerical comparisons based on a variety of such measures.

2. Measures and metrics on the rotation groups.

2.1. SO(3) as an extremely special case. The usual (angular) distance associated to a pair of rotation matrices $\mathbf{M}, \mathbf{N} \in \mathbf{SO}(3)$ is given by

$$\mathbf{d}_A(\mathbf{M}, \mathbf{N}) = \operatorname{acos}\left(\frac{1}{2}\left(\mathbf{Tr}(\mathbf{N}\mathbf{M}^{-1}) - 1\right)\right). \tag{2.1}$$

This distance formula is invariant under the group action of $\mathbf{SO}(3)$. It measures the angle of rotation needed to map the transformation $\mathbf{M}$ to the transformation $\mathbf{N}$, equivalently the angle of rotation associated to the transformation $\mathbf{N}\mathbf{M}^{-1}$. This distance metric is one of many group-invariant distance functions, but it is the only one derived from a Riemannian metric. We can define two additional (angular and Euclidean) distance functions by

$$\mathbf{d}_A(\mathbf{M}, \mathbf{N}) = \sup_{\mathbf{x} \in \mathbf{S}^2} \operatorname{acos}\left(\langle \mathbf{M}\mathbf{x}, \mathbf{N}\mathbf{x} \rangle\right) \qquad \text{and} \tag{2.2}$$

$$\mathbf{d}_E(\mathbf{M}, \mathbf{N}) = \sup_{\mathbf{x} \in \mathbf{S}^2} ||\mathbf{M}\mathbf{x} - \mathbf{N}\mathbf{x}||, \tag{2.3}$$

where $||\cdot||$ is the Euclidean norm on vectors and $\langle \cdot, \cdot \rangle$ is the Euclidean inner product. One can check that formulas (2.1) and (2.2) define identical distances on $\mathbf{SO}(3)$. Formula (2.1) does not readily extend to higher dimensional $\mathbf{SO}(n)$ as it is written, but $\mathbf{d}_A$ and $\mathbf{d}_E$ can be extended by replacing $\mathbf{S}^2$ with $\mathbf{S}^{n-1}$ in the above formulas. The distance functions $\mathbf{d}_A$ and $\mathbf{d}_E$ are distinct, but they share a natural duality.

PROPOSITION 2.1. *If* $\boldsymbol{\alpha} = \mathbf{d}_A(\mathbf{M}, \mathbf{N})$ *and* $\mathbf{s} = \mathbf{d}_E(\mathbf{M}, \mathbf{N})$ *for* $\mathbf{M}, \mathbf{N} \in \mathbf{SO}(3)$, *then*

$$\mathbf{s} = 2\ \sin\left(\frac{\boldsymbol{\alpha}}{2}\right), \quad \textit{and} \quad \boldsymbol{\alpha} = 2\ \operatorname{asin}\left(\frac{\mathbf{s}}{2}\right).$$

Proof. Define $\mathbf{u} = \mathbf{M}\mathbf{x}$ and $\mathbf{w} = \mathbf{N}\mathbf{x}$ at the point $\mathbf{x} \in \mathbf{S}^2$ for which the supremum is attained in (2.3), which must exist for a continuous function on a compact space. The proof is then explained by the geometric relationship of Figure 2.1. It is clear that the distance $\mathbf{s} = ||\mathbf{u} - \mathbf{w}||$ satisfies

$$\frac{\mathbf{s}}{2} = \sin\left(\frac{\boldsymbol{\alpha}}{2}\right),$$

and the result follows immediately. ∎

PROPOSITION 2.2. *The metrics* $\mathbf{d}_A$ *and* $\mathbf{d}_E$ *are equivalent.*

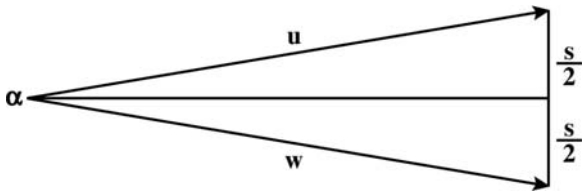

FIG. 2.1. *Duality of distance metrics. The figure indicates the reason why* $\mathbf{s} = 2\sin(\boldsymbol{\alpha}/2)$ *holds. It is clear from the figure that* $\mathbf{s}/2 = \sin(\boldsymbol{\alpha}/2)$*, and hence* $\mathbf{s} = 2\sin(\boldsymbol{\alpha}/2)$.

Proof. Let $\mathbf{s}, \boldsymbol{\alpha}$ be as in the previous proposition. Since $\boldsymbol{\alpha} \in [0, \pi]$, the ratio

$$\frac{\mathbf{s}}{\boldsymbol{\alpha}} = \frac{2\sin(\boldsymbol{\alpha}/2)}{\boldsymbol{\alpha}} = \frac{\sin(\boldsymbol{\alpha}/2)}{\boldsymbol{\alpha}/2} \tag{2.4}$$

is bounded above by 1 (near $\boldsymbol{\alpha} = 0$) and below by $2/\pi$ (near $\boldsymbol{\alpha} = \pi$). Hence, $\mathbf{d}_A$ and $\mathbf{d}_E$ define equivalent distance metrics on $\mathbf{SO}(3)$. ∎

A somewhat more important fact is that the distance metrics are nearly indistinguishable at the local scale. For the range of $\boldsymbol{\alpha}$ of interest to us, the relative error for approximating $\mathbf{d}_A$ by $\mathbf{d}_E$ is small. For example, if for some $\mathbf{M}, \mathbf{N} \in \mathbf{SO}(3)$, $\boldsymbol{\alpha} = \mathbf{d}_A(\mathbf{M}, \mathbf{N}) = \pi/12$ radians (15 degrees) and $\mathbf{s} = \mathbf{d}_E(\mathbf{M}, \mathbf{N}) = 2\sin(\alpha/2)$, the relative error in approximating $\boldsymbol{\alpha}$ by $\mathbf{s}$ is 0.00071. As $\boldsymbol{\alpha}$ tends to zero, the relative error likewise tends to zero; hence the metrics are essentially the same for small $\boldsymbol{\alpha}$. Using a Taylor expansion about $\boldsymbol{\alpha} = 0$, it is not difficult to see that

$$|\boldsymbol{\alpha} - \mathbf{s}| = |\boldsymbol{\alpha} - 2\sin\left(\frac{\boldsymbol{\alpha}}{2}\right)| = O(\boldsymbol{\alpha}^3) \quad \text{and} \quad \frac{|\boldsymbol{\alpha} - \mathbf{s}|}{|\boldsymbol{\alpha}|} = \frac{|\boldsymbol{\alpha} - 2\sin(\boldsymbol{\alpha}/2)|}{|\boldsymbol{\alpha}|} = O(\boldsymbol{\alpha}^2).$$

Thus, the relative and absolute errors for approximating $\boldsymbol{\alpha}$ by $\mathbf{s}$ are second and third order, respectively. Note that while the above formula expresses $\boldsymbol{\alpha}$ in radians we frequently express $\boldsymbol{\alpha}$ in degrees when discussing sampling resolution.

We now examine distances in a different way, in relation to the Froebenius norm on matrices. The *Froebenius norm* calculates the difference between matrices as though they were Euclidean vectors. In particular,

$$||\mathbf{M} - \mathbf{N}|| = \sqrt{\sum_{i=0}^{n-1}\sum_{j=0}^{n-1}(\mathbf{M}_{ij} - \mathbf{N}_{ij})^2}, \tag{2.5}$$

where $\mathbf{M}_{ij}$ and $\mathbf{N}_{ij}$ are the ijth elements of $\mathbf{M}$ and $\mathbf{N}$. We will henceforth use the notation $||\cdot||$ to refer to the Euclidean norm on vectors or the Froebenius norm on matrices.

PROPOSITION 2.3. *The metric* $\mathbf{d}_E$ *satisfies* $\mathbf{d}_E(\mathbf{M}, \mathbf{N}) = \frac{1}{\sqrt{2}}||\mathbf{M} - \mathbf{N}||$ *for all* $\mathbf{M}, \mathbf{N} \in \mathbf{SO}(3)$.

Proof. Planar rotations are the only case to which this proposition applies in general, and we prove the case of $\mathbf{M}, \mathbf{N} \in \mathbf{SO}(3)$. First, it is convenient to note that the Froebenius norm is invariant under an orthogonal change of coordinates; hence $||\mathbf{M} - \mathbf{N}|| = ||\ \mathbf{I} - \mathbf{N}\mathbf{M}^{-1}\ ||$. Now, suppose

$$\mathbf{N}\mathbf{M}^{-1} = \begin{bmatrix} \cos\boldsymbol{\alpha} & -\sin\boldsymbol{\alpha} & 0 \\ \sin\boldsymbol{\alpha} & \cos\boldsymbol{\alpha} & 0 \\ 0 & 0 & 1 \end{bmatrix}.$$

For $\mathbf{SO}(3)$, this can always be achieved by applying a suitable coordinate transformation. Then

$$\begin{aligned}\frac{1}{\sqrt{2}}||\ \mathbf{I}-\mathbf{N}\mathbf{M}^{-1}\ ||&=\frac{1}{\sqrt{2}}\sqrt{2(1-\cos\boldsymbol{\alpha})^2+2\sin^2\boldsymbol{\alpha}}\\&=\sqrt{(1-\cos\boldsymbol{\alpha})^2+\sin^2\boldsymbol{\alpha}}\\&=\sqrt{2-2\cos\boldsymbol{\alpha}}.\end{aligned}$$

By applying a half-angle formula, we get

$$\begin{aligned}\sqrt{2-2\cos\boldsymbol{\alpha}}&=\sqrt{2-2\cos^2(\boldsymbol{\alpha}/2)+2\sin^2(\boldsymbol{\alpha}/2)}\\&=\sqrt{4\sin^2(\boldsymbol{\alpha}/2)}\\&=2\sin(\boldsymbol{\alpha}/2)\qquad\qquad(0\le\boldsymbol{\alpha}\le\pi)\\&=\mathbf{d}_E(\mathbf{M},\mathbf{N}),\end{aligned}$$

and the fact that $\mathbf{d}_E(\mathbf{M},\mathbf{N})=\frac{1}{\sqrt{2}}||\mathbf{M}-\mathbf{N}||$ follows immediately. ∎

Thus, for $\mathbf{SO}(3)$ our distance measure $\mathbf{d}_E(\mathbf{M},\mathbf{N})$ is the same as a scaled Froebenius norm. This fact will allow us to bound distances in the proof of Theorem 2, after decomposing each rotation in $\mathbf{SO}(n)$ into a sequence of planar rotations.

2.2. A projective Euclidean metric on $\mathbf{SO}(n)$. The case of $\mathbf{SO}(3)$ is special, because there is a single angle associated to any pair of rotations, equal to their angular distance from one another. In $\mathbf{SO}(n)$, this need not be true, as exemplified when

$$\mathbf{N}\mathbf{M}^{-1}=\begin{bmatrix}\cos\boldsymbol{\alpha}_1 & -\sin\boldsymbol{\alpha}_1 & 0 & 0\\ \sin\boldsymbol{\alpha}_1 & \cos\boldsymbol{\alpha}_1 & 0 & 0\\ 0 & 0 & \cos\boldsymbol{\alpha}_2 & -\sin\boldsymbol{\alpha}_2\\ 0 & 0 & \sin\boldsymbol{\alpha}_2 & \cos\boldsymbol{\alpha}_2\end{bmatrix}.$$

Nonetheless, we can use the intuition gained from $\mathbf{SO}(3)$ to construct distance metrics on $\mathbf{SO}(n)$. To define a metric on $\mathbf{SO}(n)$, we start with the Froebenius norm, which gives a distance metric on $\mathbf{SO}(n)$ that is Euclidean in nature. This norm is related to $\mathbf{Tr}(\mathbf{N}\mathbf{M}^{-1})$ since

$$\begin{aligned}||\mathbf{M}-\mathbf{N}||^2&=\mathbf{Tr}\left((\mathbf{M}-\mathbf{N})\cdot(\mathbf{M}-\mathbf{N})^T\right)\\&=\mathbf{Tr}(\mathbf{M}\mathbf{M}^T+\mathbf{N}\mathbf{N}^T-\mathbf{M}\mathbf{N}^T-\mathbf{N}\mathbf{M}^T)\\&=2\ \mathbf{Tr}(\mathbf{I}-\mathbf{N}\mathbf{M}^T)\\&=2\ \left(n-\mathbf{Tr}(\mathbf{N}\mathbf{M}^{-1})\right).\end{aligned}$$

The norm must be scaled appropriately to obtain a correspondence with the metric defined in (2.3). The correct scaling factor, which accounts for the fact that nonunity eigenvalues of $\mathbf{N}\mathbf{M}^{-1}$ occur in complex conjugate pairs, is to define

$$\mathbf{d}(\mathbf{M},\mathbf{N})=\frac{1}{\sqrt{2}}||\mathbf{M}-\mathbf{N}||. \tag{2.6}$$

The metric $\mathbf{d}$, which we will refer to as the *projective Euclidean* metric, is nice for several reasons. First, it is invariant under the action of $\mathbf{SO}(n)$. In addition, embedding a lower dimensional $\mathbf{SO}(n)$ into a higher dimensional one does not change the

induced distance metric. Most importantly, the projective Euclidean metric leads to a Pythagorean theorem on $\mathbf{SO}(n)$, and the proof of Theorem 2 relies on this.

With this in mind, we return to the question of constructing uniform deterministic samples on $\mathbf{SO}(n)$. How do distance metrics and metric equivalences relate to Haar measure and uniform density? Equivalent distance metrics need not lead to the same probability measure. The key property needed for compatibility with the Haar measure is invariance with respect to the group. There are many group-invariant distance functions, though most do not arise from a Riemannian volume form. Non-Riemannian distance metrics can be used at the local level to ensure good nearest neighbor separation within deterministic samples, provided the metrics are group-invariant.

2.3. Measures of sampling uniformity. Uniform deterministic sampling is much more difficult than uniform random sampling. Measure-theoretic uniformity in the sense of (1.1) can be easily attained via repeated random sampling. However, the rotation sets generated in this way fail to have optimal global coverage and local separation with regard to any group-invariant distance metric.

There are many strategies for measuring the quality of uniform deterministic samples on spheres and rotation groups. We do not promote any in particular and will instead base our comparisons on several uniformity criteria.

2.3.1. Repulsive forces. Many are familiar with energy-based dispersion on $\mathbf{S}^2$ [6, 13]. For k points, $\mathbf{z}_0, \ldots, \mathbf{z}_{n-1}$, on the sphere, the goal is to optimize their positions so as to minimize a repulsive potential energy, such as

$$\mathbf{E} = \sum_{i=0}^{k-1} \sum_{j=i+1}^{k-1} ||\mathbf{z}_i - \mathbf{z}_j||^{-p} \qquad (p > 0).$$

Commonly used is the *repulsive order* $p = 1$, although we include results for a range of repulsive orders in our comparative analysis, including the 6–12 powers of relevance to Lennard–Jones clusters [23, 25, 29]. For $\mathbf{SO}(n)$, the repulsive potentials may be generalized as

$$\mathbf{E} = \sum_{i=0}^{k-1} \sum_{j=i+1}^{k-1} \mathbf{d}^{-p}(\mathbf{Z}_i, \mathbf{Z}_j), \tag{2.7}$$

where $\mathbf{Z}_i$ and $\mathbf{Z}_j$ range over a sample of the rotation space. We will see that SOI samples produce lower repulsive energies than the variable stepping and Layered Sukharev samples, and this is true across a range of repulsive orders.

2.3.2. Global coverage and local separation. In this section, we define two measures of sampling uniformity. To simplify the definitions, which must be made for both spheres and rotation groups, we will denote by $\mathbb{S}$ either of the spaces $\mathbf{S}^n$ or $\mathbf{SO}(n)$. We use the metric $\mathbf{d}$ in this section to mean the Euclidean norm if applied to a pair of vectors, or the projective Euclidean distance function if applied to elements of $\mathbf{SO}(n)$. The definitions for global coverage and local separation rely on a target angular step, $\boldsymbol{\alpha}$, and its associated length step, $\mathbf{s} = 2\sin(\boldsymbol{\alpha}/2)$.

DEFINITION 1. *A finite subset* $\mathbf{V} \subset \mathbb{S}$ *is* $(\mathbf{s}, \boldsymbol{\rho})$-covered *provided that*

$$\sup_{\mathbf{w} \in \mathbb{S}} \left(\min_{\mathbf{v} \in \mathbf{V}} \mathbf{d}(\mathbf{v}, \mathbf{w}) \right) \leq \boldsymbol{\rho} \cdot \frac{\mathbf{s}}{2} \sqrt{\dim(\mathbb{S})}.$$

This formula defines the maximum distance between an arbitrary $\mathbf{w} \in \mathbb{S}$ and a sampled point $\mathbf{v} \in \mathbf{V}$, using a regular lattice of target length step $\mathbf{s}$ to define ideality. In particular, if $\boldsymbol{\rho} \leq 1$, the upper bound is half the length of the diagonal of a cube of appropriate dimension, suggesting that the deterministic sample covers the space at least as comprehensively as a regular lattice.

DEFINITION 2. *A finite subset* $\mathbf{V}$ *of* $\mathbb{S}$ *is* $\{\mathbf{s}, \boldsymbol{\sigma}\}$-separated *provided that*

$$\max_{\mathbf{w}\in\mathbf{V}} \left(\min_{\mathbf{v}\in\mathbf{V}} \mathbf{d}(\mathbf{v}, \mathbf{w}) \right) \leq \boldsymbol{\sigma} \cdot \mathbf{s},$$
$$\min_{\mathbf{w}\in\mathbf{V}} \left(\min_{\mathbf{v}\in\mathbf{V}} \mathbf{d}(\mathbf{v}, \mathbf{w}) \right) \geq \frac{1}{\boldsymbol{\sigma}} \cdot \mathbf{s}.$$

These formulas constrain the range of nearest neighbor distances within $\mathbf{V}$. Ideally, we would like to ensure $\boldsymbol{\sigma} \approx 1$, which is true for SOI samples. The variable stepping and layered Sukharev methods both produce higher $\boldsymbol{\sigma}$ values than is desired.

2.3.3. Dispersion and discrepancy. Two common measures of sampling uniformity are *dispersion* and *discrepancy*, as defined below (see also [30, 27, 20, 22]). The case of $\mathbf{S}^2$ should be familiar to many readers, and the definitions carry over to $\mathbf{SO}(3)$.

DEFINITION 3. *A subset* $\mathbf{V} \subset \mathbb{S}$ *is* well-dispersed *provided that the supremum*

$$\sup_{\mathbf{w}\in\mathbb{S}} \left(\min_{\mathbf{v}\in\mathbf{V}} \mathbf{d}(\mathbf{v}, \mathbf{w}) \right)$$

is bounded by a quantity that depends only on the properties of the underlying space $\mathbb{S}$ *and the number of sample points in* $\mathbf{V}$.

Our definition of global coverage is nearly identical to dispersion, except that it defines a parameter that is relatively independent of the sample or step size.

DEFINITION 4. *Given a family of subsets* $\mathfrak{W} = \{\mathbf{W} \subset \mathbb{S}\}$ *and a discrete subset* $\mathbf{V} \subset \mathbb{S}$, *the* discrepancy *of* $\mathbf{V}$ *with respect to* $\mathfrak{W}$ *is*

$$\sup_{\mathbf{W}\in\mathfrak{W}} \left| \frac{|\mathbf{V} \cap \mathbf{W}|}{|\mathbf{V}|} - \frac{\boldsymbol{\mu}(\mathbf{W})}{\boldsymbol{\mu}(\mathbb{S})} \right|,$$

where $\boldsymbol{\mu}$ *is the Haar measure on* $\mathbb{S}$, $|\mathbf{V}|$ *is the cardinality of the set* $\mathbf{V}$, *and* $|\mathbf{V} \cap \mathbf{W}|$ *is the cardinality of the set* $\mathbf{V} \cap \mathbf{W}$.

Discrepancy is a useful measure, as it indicates the degree to which a deterministic sample reflects the continuous density of the underlying measure. Discrepancy describes the worst deviation between the fraction of sample points contained by a set $\mathbf{W}$ and the fraction of overall volume contained by $\mathbf{W}$. In a theoretical sense, discrepancy is most able to guarantee uniformity of a deterministic sample relative to its underlying measure. In a practical sense, it is not always straightforward to prove or estimate. There is also the matter of choosing a suitable family $\mathfrak{W}$, since including every subset of $\mathbb{S}$ would result in the maximum possible discrepancy value of 1 (consider the complements of small neighborhoods of $\mathbf{V}$ in $\mathbb{S}$).

3. SO(3) sampling schemes. The rotation group $\mathbf{SO}(3)$ can be parameterized by quaternions, Euler angles, or orthogonal matrices. Some parameterizations, such as "axis-angle," are specific to $\mathbf{SO}(3)$, whereas others generalize to higher dimensional rotation groups. Whether a parameter space can be sampled uniformly in the parameters to obtain a uniform sample of $\mathbf{SO}(3)$ depends on whether the parameterization is a local isometry. The discussion in the appendix of $\mathbf{SO}(3)$ parameterizations and their relation to Haar measure has some added details.

3.1. Uniform random sampling on SO(3). There are many ways to specify a random rotation [1, 2, 10, 21, 27, 34]. A random unit quaternion defines a uniform random rotation in $\mathbf{SO}(3)$. One can also choose random Euler angles, provided that the distributions on each angle are defined appropriately.

The subgroup algorithm for selecting random elements of a Lie group [10] is related to our SOI construction. The subgroup algorithm decomposes the process of choosing a random variable on a group $\mathbf{G}$ into a combined choice of a random element $\mathbf{h}_1 \in \mathbf{H}$ from a subgroup of $\mathbf{G}$ and an element $\mathbf{h}_2$ from the quotient or coset space.

We apply a very similar heuristic, namely, that to sample $\mathbf{SO}(3)$ uniformly with respect to the Haar measure, one can first randomly choose $\mathbf{u}_2 = \mathbf{M}\mathbf{x}_2$ as any point on the sphere $\mathbf{S}^2$. Based on the constraint that the images of orthogonal vectors must be orthogonal, we require that

$$\mathbf{u}_1 = \mathbf{M}\mathbf{x}_1 \in \mathbf{S}^2_{\perp \mathbf{u}_2} \cong \mathbf{S}^1,$$

where $\mathbf{S}^2_{\perp \mathbf{u}_2} \cong \mathbf{S}^1$ is the subset of $\mathbf{S}^2$ orthogonal to $\mathbf{u}_2$. This subspace is a ring isometric to $\mathbf{S}^1$, as in Figure 1.1. Upon choosing $\mathbf{u}_1$ uniformly from this circle, the final vector $\mathbf{u}_0 = \mathbf{M}\mathbf{x}_0$ is then uniquely determined. This procedure is the random sampling equivalent of the deterministic sampling method that we now define.

3.2. Uniform deterministic sampling on SO(3). For uniform deterministic samples, the definition of "uniform" is subject to some interpretation. Repeated random sampling, for example, is uniform in some respects but not others. Our goal is to ensure global coverage and local separation that are consistent with a lattice yet retain global uniformity of the rotation sample with regard to the Haar measure. Here, we outline a number of schemes for generating deterministic samples of $\mathbf{SO}(3)$, each of which looks at rotation space in a different way.

3.2.1. Successive Orthogonal Images. We will apply the SOI algorithm to construct a uniform deterministic sample, $\mathbf{U} \subset \mathbf{SO}(3)$, of rotation space from uniform deterministic samples, $\mathbf{V}^1 \subset \mathbf{S}^1$ and $\mathbf{V}^2 \subset \mathbf{S}^2$, on the spheres. The $\mathbf{V}^i$ can be regarded as "reference" samples, which avoids having to generate new uniform samples during the recursive process.

We will define a rotation sample by building possible combinations of mutually orthogonal unit vectors $\{\mathbf{u}_0, \mathbf{u}_1, \mathbf{u}_2\}$, where each vector represents a column of a rotation matrix, $\mathbf{M}$. To start, we define $\mathbf{U}^2 = \mathbf{V}^2$ to be the discrete set of possible choices of $\mathbf{u}_2$. Once $\mathbf{u}_2 \in \mathbf{U}^2$ has been chosen, there is one degree of freedom left with which to choose $\mathbf{u}_1$. Orthogonal constraints on the two vectors require that $\mathbf{u}_1$ lie in the subspace $\mathbf{S}^2_{\perp \mathbf{u}_2}$, a set that is isometric to the circle $\mathbf{S}^1$. Using our reference sample $\mathbf{V}^1$ as a model, we can sample this circle at a fixed length step to define possible choices for $\mathbf{u}_1$. Once $\mathbf{u}_1$ and $\mathbf{u}_2$ are specified, there is only one vector, $\mathbf{u}_0$, that can be the image of $\mathbf{x}_0$ under a transformation $\mathbf{M} \in \mathbf{SO}(3)$. This is illustrated in Figure 1.1.

To maintain the regularity of sampling, it is essential to balance the number of sample points in each subspace, in a way that is compatible with the Haar measure.

For a target angular step, $\boldsymbol{\alpha}$, we estimate that a good way to choose the size of the samples is

$$|\mathbf{V}^2| = \frac{4\pi}{\boldsymbol{\alpha}^2} \qquad \text{and} \qquad |\mathbf{V}^1| = \frac{2\pi}{\boldsymbol{\alpha}}. \tag{3.1}$$

These estimates are intended to generate samples on $\mathbf{V}^1$ and $\mathbf{V}^2$ satisfying the sampling uniformity constraints defined in section 2.3.2. The first estimate in (3.1) essentially divides the area of $\mathbf{S}^2$ into i-dimensional squares of sidelength $\boldsymbol{\alpha}$. One can envision, for example, the surface of a "disco ball" that is tiled with small square mirrors.

In fact, it is not essential that the samples resemble an actual tiling, and one can do somewhat better with a distribution such as that shown in Figure 1.1. For our calculations, we distributed points using an energy repulsion method with $p = 1$. The real goal of the estimates in (3.1) is to divide the total area of $\mathbf{S}^2$ uniformly into "parcels" of area $\boldsymbol{\alpha}^2$, while simultaneously dividing the length of $\mathbf{S}^1$ into parcels of length $\boldsymbol{\alpha}$. It is not necessary to define actual subsets of $\mathbf{S}^2$ associated to each parcel (as would be the case, for example, with a Voronoi diagram [3, 11, 28]). Instead, the formulas merely suggest the correct number of sample points needed to maintain a volumetric balance when defining a (local) product space. This balance is key to ensuring uniformity with regard to the Haar measure on $\mathbf{SO}(3)$. A volume of approximately $\boldsymbol{\alpha}^3$ is associated to each point of the final rotation sample. If the sample points are fairly uniform, this has the effect of uniformly distributing the volume of $\mathbf{SO}(3)$ in parcels of $\boldsymbol{\alpha}^3$.

We debated whether to use the target length step, $\mathbf{s}$, or target angular step, $\boldsymbol{\alpha}$, in the above estimates. Intuitively, using the length step seems more appropriate, but using $\boldsymbol{\alpha}$ is correct for $\boldsymbol{\alpha} \approx \pi$. For smaller $\boldsymbol{\alpha}$, the relative difference between $\boldsymbol{\alpha}$ and $\mathbf{s}$ is $O(\boldsymbol{\alpha}^2)$, as was previously discussed. Thus, asymptotically, using one or the other makes no difference in limiting behavior, although some limits might converge from above or below according to the convention.

3.2.2. Variable stepping. In the variable stepping method [31], Euler angle triplets $\boldsymbol{\Theta} = (\boldsymbol{\theta}_1, \boldsymbol{\theta}_2, \boldsymbol{\theta}_3)$ are used to define a uniform sampling on $\mathbf{SO}(3)$. The angles $\boldsymbol{\theta}_2, \boldsymbol{\theta}_3$ are sampled at uniform intervals of the target angular step, $\boldsymbol{\alpha}$. The remaining angle, $\boldsymbol{\theta}_1$, is sampled in steps of

$$\boldsymbol{\alpha}' = \frac{\boldsymbol{\alpha}}{\sin(\boldsymbol{\theta}_2)}. \tag{3.2}$$

For cases such as $\boldsymbol{\theta}_2 = 0$ or π, where the calculated step exceeds 2π, only $\boldsymbol{\theta}_1 = 0$ is sampled.

The reasoning behind this construction is quite simple. The angles $\boldsymbol{\theta}_1$ and $\boldsymbol{\theta}_2$ determine $\mathbf{u}_2 = \mathbf{M}\mathbf{x}_2$, per the formula given in the appendix. The distribution of the $\mathbf{u}_2$ vectors should be uniform on the unit sphere. Now, unit great circle $\boldsymbol{\theta}_2 = \frac{\pi}{2}$ has circumference 2π, and the set of all points with a constant value of $\boldsymbol{\theta}_2$ forms a circle of circumference $2\pi \cdot \sin(\boldsymbol{\theta}_2)$, including the trivial cases $\boldsymbol{\theta}_2 = 0, \pi$. The ratio of points sampled on the two circles should be the ratio of their lengths,

$$\frac{2\pi \cdot \sin(\frac{\pi}{2})}{2\pi \cdot \sin(\boldsymbol{\theta}_2)} = \frac{1}{\sin(\boldsymbol{\theta}_2)},$$

and formula (3.2) follows.

The variable stepping method gives good global coverage of the space, and it is fairly uniform. The method does exhibit some lack of local separation in the sample points, as will be seen in the numerical results of section 3.3.

3.2.3. Hierarchical generation. Another asymptotically convergent method for generating dispersed samples of $\mathbf{SO}(3)$ is hierarchical generation [18]. The hierarchical generation method uses three generators, $\mathbf{T}_1, \mathbf{T}_2, \mathbf{T}_3$, each of which rotates about one of the principal axes by an angle of $\boldsymbol{\alpha} = \operatorname{acos}(-\frac{3}{5})$. Let $\mathbf{T}_6, \mathbf{T}_5, \mathbf{T}_4$ be their respective inverses, so that $\mathbf{T}_{i_1} = \mathbf{T}_{i_2}^{-1}$ when $i_1 + i_2 = 7$. An order k sample consists of all products, $\mathbf{T} = \mathbf{T}_{i_1} \cdots \mathbf{T}_{i_k}$, such that $(i_j + i_{j+1}) \neq 7$ for any j. The total number of matrices generated for an order j sample is $k = 6 + (6 \cdot 5) + (6 \cdot 5^2) + \cdots + (6 \cdot 5^{j-1}) = \frac{3}{2} \cdot (5^j - 1)$. The hierarchical generation method is useful in situations where a very large number of well-dispersed rotations is needed. Because of the limited control over rotation sample sizes, which grow exponentially, we do not include this method in our numerical comparisons.

3.2.4. Layered Sukharev grids. The layered Sukharev method samples rotation space using Sukharev spherical grids [33]. Grids are constructed on the faces of a cube in $(n+1)$-dimensional space and projected onto $\mathbf{S}^n$. By regarding $\mathbf{S}^3$ as a double cover of $\mathbf{SO}(3)$, the method has also been applied to three-dimensional rotations.

A nice feature of the layered Sukharev method is its ability to incrementally add sample points on layered sampling grids. The method is distinct in this respect, relative to others described in this section. In addition, it produces a grid-like network of sample points. These aspects have made it useful in motion planning applications [33]. Layered Sukharev grids are coarsely uniform and very grid-like, but they will converge asymptotically to a distribution that is denser in some areas than others (essentially in the same way that a cube does not project uniformly onto a sphere).

3.2.5. Frame axis-angle. Like SOI, the frame axis-angle (FAA) representation [17, 32] poses the question of sampling the rotation group by combining uniform deterministic samples of $\mathbf{S}^1$ and $\mathbf{S}^2$ into a sample of $\mathbf{SO}(3)$. The published applications seem to use a sampling heuristic that is equivalent to applying the SOI construction with a sample $\mathbf{V}^2$ derived from Sukharev or similar, spherical grids. The asymptotic case gives a nonuniform density, for the same reasons as with the layered Sukharev method.

FAA is different from the layered Sukharev method, which uses Sukharev grids in $\mathbb{R}^4$ projected to quaternions in $\mathbf{S}^3$ and then mapped to rotations in $\mathbf{SO}(3)$. Although distinct, the method's use of spherical grids is apt to produce comparable numerical results, due to the nonuniformity of nearest neighbor distances within the sample. For brevity, we include only the layered Sukharev method in our direct comparisons.

3.3. Numerical results. Rotation samples were generated for the SOI and variable stepping methods at angular steps $\boldsymbol{\alpha} = 4, 6, 8, 10, 12, 15$ degrees. For each target angular step, Table 3.1 shows the target length step $\mathbf{s}$ and the sizes of the sets $\mathbf{V}^1, \mathbf{V}^2$, and $\mathbf{U}$ as defined in the SOI construction. For our numerical comparisons, we generated $\mathbf{V}^1$ and $\mathbf{V}^2$ by optimizing a repulsive potential with $p = 1$. Layered Sukharev samples are based on the number of sample points, and the SOI sample sizes were used to obtain an equal comparison between the methods.

We will examine how the samples perform with regard to various uniformity criteria, starting with energy repulsion. Pairwise repulsive energies were calculated for all rotation samples, and SOI samples produced lower repulsive energies than the other two methods. This was true at all length steps and for a range of repulsive orders.

TABLE 3.1
For each target angular step $\boldsymbol{\alpha}$ (in degrees), the table gives the target length step, $\mathbf{s}$, along with the number of points in $\mathbf{V}^1$, $\mathbf{V}^2$, and $\mathbf{U}$ for the SOI sample.

$\boldsymbol{\alpha}$	$\mathbf{s}$	$\lvert\mathbf{V}^1\rvert$	$\lvert\mathbf{V}^2\rvert$	$\lvert\mathbf{U}\rvert$
4	0.07	90	2578	232020
6	0.10	60	1146	68760
8	0.14	45	645	29025
10	0.17	36	413	14868
12	0.21	30	286	8580
15	0.26	24	183	4392

In addition, global coverage and local separation were analyzed for each deterministic sample. In each case, the SOI method produced the most uniform distributions. The numerical results demonstrate the following.

- The SOI method produces *lower repulsive potential energies* than either layered Sukharev or variable stepping (Table 3.2).
- The *global coverage and local separation properties* of SOI samples are nearly optimal (Figure 3.1(a)).
- SOI coverage *mimics a lattice* in certain respects. This is shown by generating a profile of random nearest neighbor distances (Figure 3.1(b)).
- SOI achieves a *nearly perfect distribution of nearest neighbor distances* between sample points (Figure 3.2).

3.3.1. Repulsive energies. The SOI, layered Sukharev and variable stepping methods are compared with respect to their repulsive energies in Table 3.2. The total repulsive energies were calculated for repulsive orders $p \in \left\{\frac{1}{2}, 1, 2, 3, 6, 12\right\}$ using the formula given in (2.7). The cases $p = 1, 2, 3$ are of interest in potential theory, and $p = 6, 12$ are relevant to the study of Lennard–Jones clusters [23, 25, 29]. In each case, the SOI samples produced the lowest repulsive energies.

For a given value of p and a target angular step, $\boldsymbol{\alpha}$, we considered the absolute and relative differences between the repulsive energies of the SOI samples and those of variable stepping or layered Sukharev. Smaller repulsive orders ($p = 1, 2, 3$) produced relative differences of as much as 5%–38%, depending on the repulsive order. As the sampling became finer, the relative differences tended to increase. This effect was most pronounced for the 6–12 powers, for which there were many orders of magnitude differences in the repulsive energies. These results suggest that the local spacing of SOI samples is much more precise than for the other two methods, which is supported by the local separation results presented in the next section.

3.3.2. Global coverage and local separation. SOI samples achieve good global coverage of the rotation group. A fundamental goal of uniform sampling is to define a discrete set, $\mathbf{U}$, of fixed size for which the dispersion

$$\sup_{\mathbf{M}\in\mathbf{SO}(n)} \left(\min_{\mathbf{N}\in\mathbf{U}} \mathbf{d}(\mathbf{M}, \mathbf{N}) \right) \tag{3.3}$$

is minimized. This formula defines a Hausdorff distance between $\mathbf{SO}(n)$ and its discrete subset $\mathbf{U}$. It can be interpreted as bounding the size of the largest "hole" in the coverage given by the discrete sample. Equivalently, it gives the radius of the largest ball that can fit inside the complement (within $\mathbf{SO}(n)$) of the discrete subset $\mathbf{U}$.

For the rotation samples described in Table 3.2, we calculated the global coverage parameter, $\boldsymbol{\rho}$, a constant multiple of which bounds the supremum (3.3) according

TABLE 3.2

The table reports the absolute and relative differences in energy (E) values for the layered Sukharev (LS) and variable stepping (VS) methods with Successive Orthogonal Images (SOI). Target angular steps of $4, 6, 8, 10, 12, 15$ *degrees are analyzed. The rightmost columns represent different values of p, the exponent used to define repulsive potentials in* (2.7)*. In absolute terms, there are considerable differences in repulsive energy for samples generated by layered Sukharev or variable stepping as compared with SOI. In relative terms, the difference is as much as* 5%–38% *for low-order exponents. For finer samples and larger p, the differences are measured in orders of magnitude.*

Absolute diff.	$\boldsymbol{\alpha}$	$p = 0.5$	1.0	2.0	3.0	6.0	12.0
Layered Sukharev	4	8.413e+05	8.511e+06	1.109e+08	2.392e+09	8.419e+13	3.923e+23
	6	3.271e+05	1.100e+06	1.533e+07	1.666e+08	7.845e+11	5.149e+19
	8	1.959e+05	8.442e+05	3.655e+06	3.907e+07	1.667e+11	1.207e+19
$(e_{LS} - e_{SOI})$	10	4.081e+05	4.747e+05	9.870e+05	5.064e+06	3.084e+09	2.754e+15
	12	7.967e+04	8.214e+04	3.506e+05	2.411e+06	1.501e+09	1.355e+15
	15	6.289e+03	3.217e+04	2.176e+05	7.615e+05	4.713e+08	4.914e+14
Variable stepping	4	1.656e+04	3.138e+06	2.449e+07	9.090e+07	5.008e+12	6.913e+22
	6	1.566e+05	5.197e+05	3.836e+06	1.910e+07	5.285e+10	4.113e+18
	8	1.847e+05	1.021e+06	2.827e+06	1.555e+07	8.800e+11	1.566e+22
$(e_{VS} - e_{SOI})$	10	5.220e+05	6.112e+05	1.113e+06	1.957e+06	2.157e+09	3.599e+16
	12	6.884e+05	7.539e+05	1.061e+06	1.634e+06	2.409e+09	7.396e+16
	15	2.181e+05	1.283e+05	7.260e+04	2.704e+05	2.167e+08	9.550e+14
Relative diff.	$\boldsymbol{\alpha}$	$p = 0.5$	1.0	2.0	3.0	6.0	12.0
Layered Sukharev	4	1.254e-02	5.432e-02	1.193e-01	3.782e-01	1.155e+01	9.986e+03
	6	7.931e-03	1.483e-02	8.012e-02	2.436e-01	3.982e+00	5.719e+02
	8	5.713e-03	2.069e-02	5.572e-02	2.758e-01	1.111e+01	9.941e+03
$\frac{(E_{LS}-E_{SOI})}{E_{SOI}}$	10	1.494e-02	1.731e-02	3.571e-02	1.219e-01	1.515e+00	6.436e+01
	12	4.241e-03	4.425e-03	2.505e-02	1.554e-01	3.805e+00	4.907e+02
	15	8.544e-04	5.412e-03	4.807e-02	1.604e-01	8.797e+00	4.964e+03
Variable stepping	4	2.468e-04	2.003e-02	2.635e-02	1.437e-02	6.870e-01	1.759e+03
	6	3.798e-03	7.005e-03	2.005e-02	2.793e-02	2.683e-01	4.568e+01
	8	5.387e-03	2.501e-02	4.310e-02	1.098e-01	5.862e+01	1.290e+07
$\frac{(E_{VS}-E_{SOI})}{E_{SOI}}$	10	1.911e-02	2.229e-02	4.026e-02	4.711e-02	1.060e+00	8.411e+02
	12	3.664e-02	4.062e-02	7.581e-02	1.054e-01	6.107e+00	2.678e+04
	15	2.963e-02	2.158e-02	1.604e-02	5.694e-02	4.046e+00	9.647e+03

to the formulas in Definition 1 of section 2.3.2. In addition, we calculated the local separation parameter, $\boldsymbol{\sigma}$. We see that SOI samples lie in the target region with $\boldsymbol{\sigma} \approx 1$ and $\boldsymbol{\rho} \leq 1$ (Figure 3.1(a)).

In addition to bounding (3.3), it is interesting to analyze the distribution of distances achieved by choosing $\mathbf{M}$ randomly. A *random nearest neighbor distance* will denote the minimum distance between a (uniformly) random element $\mathbf{M} \in \mathbf{SO}(n)$ and an element $\mathbf{N} \in \mathbf{U}$ of the deterministic sample. By repeatedly calculating random nearest neighbor distances, we obtain an idea of the global coverage and generate statistics on the distribution of nearest neighbor distances at the local level. Figure 3.1(b) compares the distribution of random nearest neighbor distances with those obtained on a regular lattice. The lattice random distances are calculated by sorting 10,000 random nearest neighbor distances on a lattice of length step $\mathbf{s} = 2\sin(\boldsymbol{\alpha}/2) \approx 0.07$, or $\boldsymbol{\alpha} = 4$ degrees. The $\mathbf{SO}(3)$ random distances are taken from 10,000 nearest neighbor distances (within $\mathbf{SO}(3)$) for a deterministic sample of target angular step $\boldsymbol{\alpha}$.

One cannot achieve a perfect correlation between the $\mathbf{SO}(3)$ random distances and the lattice random distances, due to $\mathbf{SO}(3)$ curvature. However, the SOI and variable stepping methods achieve excellent correlation, with deviation at the farthest distances, where differences arise between lattice-like and packing-like arrangements and between flat and curved spaces. That the local coverage of the sample is comparable to a lattice is established in a statistical sense, by correlation with the distribution of lattice random distances. Though results are shown only for the specific case where $\boldsymbol{\alpha} = 4$ degrees, the correlation was typical of that observed for all target angular steps.

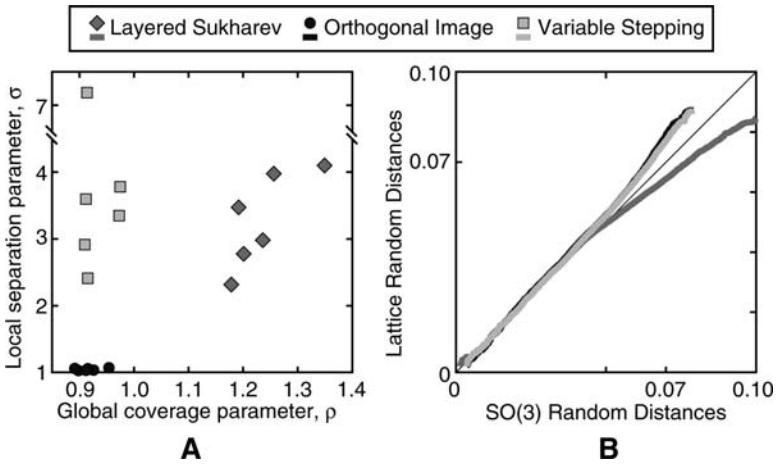

FIG. 3.1. *Tests of global coverage.* (a) *The plot shows calculated values for the global coverage and local separation measures,* $\boldsymbol{\sigma}$ *and* $\boldsymbol{\rho}$*, for rotation samples taken at step length* $\boldsymbol{\alpha} = 4, 6, 8, 10, 15$ *degrees. Symbols and shades for each method are shown in the legend. The optimal region has* $\boldsymbol{\sigma} \approx 1$ *and* $\boldsymbol{\rho} \leq 1$*. The condition* $\boldsymbol{\sigma} \approx 1$ *ensures that nearest neighbor distances are very near to the angular step, whereas* $\boldsymbol{\rho} \leq 1$ *ensures that there are no gaps in the global coverage (i.e., the sample is well dispersed).* (b) *Random nearest neighbor distances are compared for samples of* $\mathbf{SO}(3)$ *and a regular lattice, using* $10,000$ *random rotations or points. Each random rotation (or point) has a nearest neighbor in* $\mathbf{SO}(3)$ *(or the lattice). The correlation between the distributions of neighbor distance suggests whether a rotation sample is lattice-like in this regard. The variable stepping and SOI methods produce the best correlations. Perfect correlations cannot be obtained, and effect of curvature is evident at larger distances.*

We also considered pairwise nearest neighbor distances entirely within $\mathbf{U}$, to ensure that local separation was comparable to the target length step. For each sample point, its nearest neighbor distance to any other sample point was calculated. The minimum and maximum such distances were then compared against the target length step. Both the minimum and maximum separation distances for SOI distributions align nicely with the target length step, and the distribution of separation distances is nearly optimal (Figure 3.2). This is another sense in which our samples resemble a regular lattice, which has perfectly uniform nearest neighbor spacing.

4. Successive Orthogonal Image sampling on $\mathbf{SO}(n)$. We will construct uniform deterministic samples of $\mathbf{SO}(n)$ using uniform deterministic samples of the spheres, $\mathbf{S}^k$, for $k < n$. To do this, a transformation $\mathbf{M} \in \mathbf{SO}(n)$ will be defined by the orthogonal images, $\mathbf{u}_i = \mathbf{M}\mathbf{x}_i$, of the principal unit vectors, $\mathbf{x}_i$. We use a target angular step, $\boldsymbol{\alpha}$, and associated length step, $\mathbf{s}$, to define the sampling rate. These continue to share the relationship $\mathbf{s} = 2\sin(\boldsymbol{\alpha}/2)$, but they are no longer identical to the Riemannian and projective Euclidean metrics except in the case of a planar rotation.

4.1. Generalized Successive Orthogonal Image construction. To construct an SOI sample, first choose $\mathbf{u}_{n-1} = \mathbf{M}\mathbf{x}_{n-1}$ from a uniform deterministic sample $\mathbf{U}^{n-1} \subset \mathbf{S}^{n-1}$. Next, $\mathbf{u}_{n-2} = \mathbf{M}\mathbf{x}_{n-2}$ is chosen from a uniform deterministic sample $\mathbf{U}^{n-2} \subset \mathbf{S}^{n-1}_{\perp \mathbf{u}_{n-1}} \cong \mathbf{S}^{n-2}$. Continuing, $\mathbf{u}_{n-3} = \mathbf{M}\mathbf{x}_{n-3}$ is chosen from $\mathbf{U}^{n-3} \subset \mathbf{S}^{n-1}_{\perp\{\mathbf{u}_{n-2}, \mathbf{u}_{n-1}\}} \cong \mathbf{S}^{n-3}$. This process continues until $\mathbf{u}_1 = \mathbf{M}\mathbf{x}_1$ has been chosen from a uniform sample $\mathbf{U}^1$ on $\mathbf{S}^{n-1}_{\perp\{\mathbf{u}_2, \ldots, \mathbf{u}_{n-1}\}} \cong \mathbf{S}^1$, after which $\mathbf{u}_0 = \mathbf{M}\mathbf{x}_0$ is

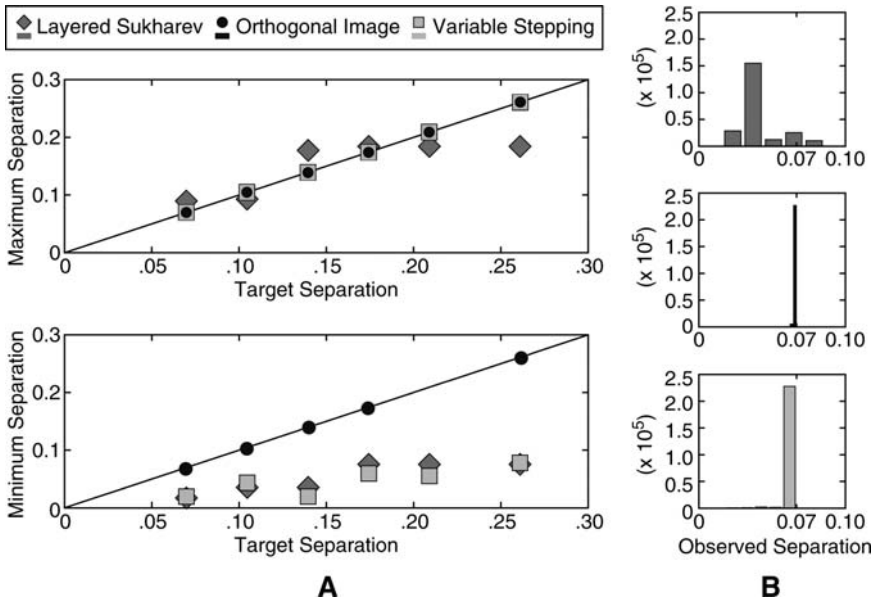

FIG. 3.2. *Local separation of rotation samples.* (a) *The two plots show the target separation distance,* $\mathbf{s} = 2\sin(\boldsymbol{\alpha}/2)$*, in relation to the minimum and maximum observed nearest neighbor separation distances for all the rotation samples analyzed in Table* 3.2*. Symbols and shades for each method are shown in the legend. SOI samples achieve nearly perfect separation.* (b) *The histograms show the distribution of nearest neighbor distances for each method on a fine rotation sample (*$\boldsymbol{\alpha} = 4$ *degrees,* $\mathbf{s} \approx 0.07$*). SOI samples produce very tight distributions near the target separation distance. The variable stepping method also produces nearest neighbor distances that are near to the target length step, with a few that are spaced too closely.*

determined. The set $\mathbf{S}^{n-1}_{\perp\{\mathbf{u}_1,\ldots,\mathbf{u}_{n-1}\}}$ contains only two vectors, only one of which can be chosen as $\mathbf{u}_0$ if $\mathbf{M}$ is to lie in $\mathbf{SO}(3)$. Note, however, that the sampling results carry over immediately to $\mathbf{O}(3)$ by sampling both $\mathbf{u}_0$ and $-\mathbf{u}_0$ as a final step.

The construction can be summarized by the following formula, which is satisfied recursively, starting from $i = (n-1)$ and working backward to $i = 1$:

$$\mathbf{u}_i \in \mathbf{U}^i \subset \mathbf{S}^{n-1}_{\perp\{\mathbf{u}_{i+1},\ldots,\mathbf{u}_{n-1}\}} \cong \mathbf{S}^i. \tag{4.1}$$

For example, in $\mathbf{SO}(3)$ one selects $\mathbf{u}_2 \in \mathbf{U}^2 \subset \mathbf{S}^2$, followed by $\mathbf{u}_1 \in \mathbf{U}^1 \subset \mathbf{S}^2_{\perp\mathbf{u}_2} \cong \mathbf{S}^1$. The space $\mathbf{S}^2_{\perp\{\mathbf{u}_1,\mathbf{u}_2\}}$ consists of two points, only one of which will make $\mathbf{M}$ into an orientation preserving transformation; hence $\mathbf{u}_0 = \mathbf{u}_1 \times \mathbf{u}_2$ is uniquely determined.

In all this, we have obscured an important detail. The sets $\mathbf{U}^i$ are defined relative to a choice of $\{\mathbf{u}_{i+1},\ldots,\mathbf{u}_{n-1}\}$. However, it is not essential to calculate a uniform deterministic sample at each stage, only to map appropriately chosen samples $\mathbf{V}^i \subset \mathbf{S}^i$ to $\mathbf{U}^i \subset \mathbf{S}^{n-1}_{\perp\{\mathbf{u}_{i+1},\ldots,\mathbf{u}_{n-1}\}}$, according to the orthogonality constraints in (4.1). The maps $\boldsymbol{\psi}_{\{\mathbf{u}_{i+1},\ldots,\mathbf{u}_{n-1}\}} : \mathbf{S}^i \to \mathbf{S}^{n-1}_{\perp\{\mathbf{u}_{i+1},\ldots,\mathbf{u}_{n-1}\}}$ for which $\boldsymbol{\psi}_{\{\mathbf{u}_{i+1},\ldots,\mathbf{u}_{n-1}\}}(\mathbf{V}^i) = \mathbf{U}^i$ are not uniquely determined. In fact, the space of possible $\boldsymbol{\psi}_{\{\mathbf{u}_{i+1},\ldots,\mathbf{u}_{n-1}\}}$ is isomorphic to $\mathbf{SO}(i+1)$. This is of little consequence to us, aside from providing added evidence that our sampling is invariant under group actions. What matters for the construction is only that the $\boldsymbol{\psi}_{\{\mathbf{u}_{i+1},\ldots,\mathbf{u}_{n-1}\}}$ exist. The proofs of Theorems 1 and 2 do not rely on any particular choice of $\boldsymbol{\psi}_{\{\mathbf{u}_{i+1},\ldots,\mathbf{u}_{n-1}\}}$, only that the samples used in (4.1) are uniform in the sense defined in section 2.3.2. In particular, the following definition

leads to nice sampling uniformity results.

DEFINITION 5. *An $\{\mathbf{s}, \boldsymbol{\rho}, \boldsymbol{\sigma}\}$-orthogonal sample is defined to be a uniform deterministic sample $\mathbf{U} \subset \mathbf{SO}(n)$ constructed from a sequence of uniform deterministic samples $\mathbf{V}^i \subset \mathbf{S}^i$ that are $\{\mathbf{s}, \boldsymbol{\rho}\}$-covered and $\{\mathbf{s}, \boldsymbol{\sigma}\}$-separated, as follows:*

$$\mathbf{u}_{n-1} \in \mathbf{U}^{n-1}, \quad \mathbf{u}_{n-2} \in \mathbf{U}^{n-2}_{\perp \mathbf{u}_{n-1}}, \quad \mathbf{u}_{n-3} \in \mathbf{U}^{n-3}_{\perp \{\mathbf{u}_{n-2}, \mathbf{u}_{n-1}\}}, \quad \ldots, \quad \mathbf{u}_1 \in \mathbf{U}^{1}_{\perp \{\mathbf{u}_2, \ldots, \mathbf{u}_{n-1}\}},$$

where the transformations $\boldsymbol{\psi}_{\{\mathbf{u}_{i+1}, \ldots, \mathbf{u}_{n-1}\}} : \mathbf{S}^i \to \mathbf{S}^{n-1}_{\perp \{\mathbf{u}_{i+1}, \ldots, \mathbf{u}_{n-1}\}}$ are isometries with $\boldsymbol{\psi}_{\{\mathbf{u}_{i+1}, \ldots, \mathbf{u}_{n-1}\}}(\mathbf{V}^i) = \mathbf{U}^i_{\perp \{\mathbf{u}_{i+1}, \ldots, \mathbf{u}_{n-1}\}}$. The $\mathbf{U}^i = \mathbf{U}^i_{\perp \{\mathbf{u}_{i+1}, \ldots, \mathbf{u}_{n-1}\}}$ are subsets of $\mathbf{S}^{n-1}$ contained in subspaces, $\mathbf{S}^{n-1}_{\perp \{\mathbf{u}_{i+1}, \ldots, \mathbf{u}_{n-1}\}}$, that are isomorphic to $\mathbf{S}^i$ and orthogonal to $\{\mathbf{u}_{i+1}, \ldots, \mathbf{u}_{n-1}\}$.

Generalizing the case of $\mathbf{SO}(3)$, a good estimate for the number of points to choose in each $\mathbf{V}^i$ is

$$|\mathbf{V}^i| \approx \frac{|\mathbf{S}^i|}{\boldsymbol{\alpha}^i},$$

where $|\mathbf{S}^i|$ is the i-dimensional volume of $\mathbf{S}^i$. The total size of a SOI sample $\mathbf{U}$ is

$$|\mathbf{U}| \approx \prod_{i=1}^{n-1} |\mathbf{V}^i| = \prod_{i=1}^{n-1} \frac{|\mathbf{S}^i|}{\boldsymbol{\alpha}^i} = \frac{1}{\boldsymbol{\alpha}^m} \prod_{i=1}^{n-1} |\mathbf{S}^i|,$$

where $m = \frac{n(n-1)}{2}$ is the topological dimension of $\mathbf{SO}(n)$. This formula gives the volume of $\mathbf{SO}(n)$ divided by the volume of an m-dimensional cube of sidelength $\boldsymbol{\alpha}$.

4.2. Analytic uniformity results. Here, we consider the general case of $\mathbf{SO}(n)$, starting with a target nearest neighbor angular spacing, $\boldsymbol{\alpha}$, and its associated length step, $\mathbf{s} = 2\sin(\boldsymbol{\alpha}/2)$. The layered Sukharev and variable stepping methods have not been extended to higher dimensional $\mathbf{SO}(n)$, so numerical comparisons are not possible. Nonetheless, we can prove bounds on the global coverage and local separation of SOI samples in these higher dimensional spaces. Bounds are established by controlling the global coverage and local separation of the $\mathbf{V}^i$, as in Definition 5.

We again stress a key difference between the general case and that of $\mathbf{SO}(3)$. Elements of $\mathbf{SO}(3)$ are all planar rotations. The definitions given in (2.2) and (2.3) carry over to general $\mathbf{SO}(n)$, but they may differ from the Riemannian and projective Euclidean distance metrics. In particular, the result of Proposition 2.3 applies only to planar rotations. We also reiterate that the use of non-Riemannian distance metrics does not impact our ability to distribute points uniformly with regard to the Haar measure. All distance metrics we consider are group-invariant. In addition, they are equivalent to the group-invariant Riemannian distance metric, which ensures they are relatively well behaved.

To prove analytic results for SOI samples, we decompose any element of $\mathbf{SO}(n)$ into a sequence of planar rotations. Norms on these planar rotations are easily characterized, per the above discussion. If two matrices, $\mathbf{M}, \mathbf{N} \in \mathbf{SO}(n)$, differ by a planar rotation, then $\mathbf{d}(\mathbf{M}, \mathbf{N}) \leq \mathbf{s}$ precisely when $\boldsymbol{\delta}(\mathbf{M}, \mathbf{N}) \leq \boldsymbol{\alpha}$, where $\boldsymbol{\delta}$ is the group-invariant Riemannian distance metric on $\mathbf{SO}(n)$. Thus, we can define optimal distances and bounds in terms of $\mathbf{s}$ and $\mathbf{d}$, rather than $\boldsymbol{\alpha}$ and $\boldsymbol{\delta}$.

Theorem 1 establishes the local separation properties of SOI samples, based on the properties of the uniform samples $\mathbf{V}^i \subset \mathbf{S}^i$. Local separation defines upper and lower bounds on pairwise nearest neighbor distances within the deterministic sample.

At the local level, the chosen constraints are intended to mirror those of a regular lattice in $\mathbb{R}^m$.

Theorem 2 establishes the global coverage properties of SOI deterministic samples, which likewise depend on the global coverage properties of the $\mathbf{V}^i$. An upper bound is attained for the maximum distance between any point in $\mathbf{SO}(n)$ and a point in the rotation sample. Constraints are again based on the properties of a regular lattice of length step $\mathbf{s}$.

In what follows, it will be useful to think of the matrix $\mathbf{NM}^{-1}$ as being defined by the vectors $\{\mathbf{u}_i = \mathbf{M}\mathbf{x}_i\}$ and $\{\mathbf{w}_i = \mathbf{N}\mathbf{x}_i\}$, as in previous sections. The construction we use for the proof of Theorem 2 will make use of vectors, $\mathbf{v}_i$, that are intermediates between $\mathbf{u}_i$ and $\mathbf{w}_i$ when constructing $\mathbf{NM}^{-1}$. This can be understood both geometrically and numerically. Working backward from $i = n-1$, the maps from $\mathbf{v}_i$ to $\mathbf{w}_i$ define a matrix decomposition into planar rotations acting within progressively smaller subspaces of $\mathbb{R}^n$. This decomposition is unique except in the case where $\mathbf{v}_i = -\mathbf{w}_i$ for some i.

4.2.1. Proof of local separation.

THEOREM 1. *An $\{\mathbf{s}, \boldsymbol{\rho}, \boldsymbol{\sigma}\}$-orthogonal sample $\mathbf{U} \subset \mathbf{SO}(n)$ is $\{\mathbf{s}, \boldsymbol{\sigma}\}$-separated.*

Proof. We must demonstrate that

$$\text{(a)} \quad \min_{\mathbf{M}\in\mathbf{U}} \left(\min_{\mathbf{N}\in\mathbf{U}-\{\mathbf{M}\}} \mathbf{d}(\mathbf{M},\mathbf{N}) \right) \geq \frac{1}{\boldsymbol{\sigma}} \cdot \mathbf{s},$$

$$\text{(b)} \quad \max_{\mathbf{M}\in\mathbf{U}} \left(\min_{\mathbf{N}\in\mathbf{U}-\{\mathbf{M}\}} \mathbf{d}(\mathbf{M},\mathbf{N}) \right) \leq \boldsymbol{\sigma} \cdot \mathbf{s}.$$

Proof of (a). The proof proceeds by contradiction. For the first statement, suppose it is false. Then for some $\mathbf{M} \in \mathbf{U}$, its nearest neighbor $\mathbf{N} \in \mathbf{U} - \{\mathbf{M}\}$ has distance $\mathbf{d}(\mathbf{M},\mathbf{N}) < \frac{1}{\boldsymbol{\sigma}} \cdot \mathbf{s}$. This implies for $i = 1, \ldots, n-1$ that

$$||\mathbf{u}_i - \mathbf{w}_i|| \leq \mathbf{d}(\mathbf{M},\mathbf{N}) < \frac{1}{\boldsymbol{\sigma}} \cdot \mathbf{s}. \tag{4.2}$$

It may first seem that there is a factor of two missing from the equation above, but the statement is correct. The transformation $\mathbf{NM}^{-1}$ will move a pair of vectors, each by at least $||\mathbf{u}_i - \mathbf{w}_i||$. It follows that $2||\mathbf{u}_i - \mathbf{w}_i||^2 \leq ||\mathbf{M} - \mathbf{N}||^2$, and so $||\mathbf{u}_i - \mathbf{w}_i|| \leq \mathbf{d}(\mathbf{M},\mathbf{N})$, using (2.6).

Now, each $\mathbf{U}^i$ is $\{\mathbf{s}, \boldsymbol{\sigma}\}$-separated by definition, and so (4.2) implies $||\mathbf{u}_i - \mathbf{w}_i|| = 0$ for $i = 1, \ldots, n-1$. It follows that $\mathbf{M} = \mathbf{N}$, because elements of $\mathbf{SO}(n)$ that are identical in their last $(n-1)$ columns are identical in the first column as well. This is a contradiction, since we assumed that $\mathbf{N} \in \mathbf{U} - \{\mathbf{M}\}$, and so (a) must be true.

Proof of (b). It is sufficient to show that for each $\mathbf{M} \in \mathbf{U}$, there exists an element $\mathbf{N} \in \mathbf{U} - \{\mathbf{M}\}$ for which $\mathbf{d}(\mathbf{M},\mathbf{N}) \leq \boldsymbol{\sigma} \cdot \mathbf{s}$. By construction of $\mathbf{U}$, there exists $\mathbf{N} \in \mathbf{U}$ for which $\mathbf{u}_j = \mathbf{w}_j$ for $j = 2, \ldots, n-1$. There is a subgroup isomorphic to $\mathbf{S}^1$ from which to choose $\mathbf{w}_1$. Because the sampling of this subgroup is $\{\mathbf{s}, \boldsymbol{\sigma}\}$-separated by assumption, this vector can be chosen to satisfy $0 < ||\mathbf{u}_1 - \mathbf{w}_1|| \leq \boldsymbol{\sigma} \cdot \mathbf{s}$.

The transformation $\mathbf{NM}^{-1}$ will leave invariant all but the plane defined by $\mathbf{x}_0$ and $\mathbf{x}_1$, since $\mathbf{M}\mathbf{x}_i = \mathbf{N}\mathbf{x}_i$ for $2 \leq i \leq n-1$. In addition, it is clear that

$$||\mathbf{u}_0 - \mathbf{w}_0|| = ||\mathbf{u}_1 - \mathbf{w}_1||.$$

All other distances are trivial, since $||\mathbf{u}_i - \mathbf{w}_i|| = 0$ for $2 \le i \le n-1$. From this, we may conclude that

$$\begin{aligned}\mathbf{d}(\mathbf{M},\mathbf{N}) &= \frac{1}{\sqrt{2}}||\mathbf{M}-\mathbf{N}|| \\ &= \frac{1}{\sqrt{2}}\sqrt{||\mathbf{M}\mathbf{x}_0 - \mathbf{N}\mathbf{x}_0||^2 + ||\mathbf{M}\mathbf{x}_1 - \mathbf{N}\mathbf{x}_1||^2} \\ &= \frac{1}{\sqrt{2}}\sqrt{||\mathbf{u}_0 - \mathbf{w}_0||^2 + ||\mathbf{u}_1 - \mathbf{w}_1||^2} \\ &= \frac{1}{\sqrt{2}}\sqrt{2||\mathbf{u}_1 - \mathbf{w}_1||^2} \\ &= ||\mathbf{u}_1 - \mathbf{w}_1|| \\ &\le \boldsymbol{\sigma}\cdot\mathbf{s},\end{aligned}$$

and the result follows. ∎

4.2.2. Proof of global coverage.

THEOREM 2. *An $\{\mathbf{s},\boldsymbol{\rho},\boldsymbol{\sigma}\}$-orthogonal sample on $\mathbf{U}\subset\mathbf{SO}(n)$ is $\{\mathbf{s},\boldsymbol{\rho}\}$-covered.*

Proof. We must demonstrate that

$$\sup_{\mathbf{M}\in\mathbf{SO}(n)}\left(\min_{\mathbf{N}\in\mathbf{U}}\mathbf{d}(\mathbf{M},\mathbf{N})\right) \le \boldsymbol{\rho}\cdot\frac{\mathbf{s}}{2}\sqrt{m}, \tag{4.3}$$

where $m = \frac{n(n-1)}{2}$ is the topological dimension of $\mathbf{SO}(n)$. In other words, given an arbitrary $\mathbf{M}\in\mathbf{SO}(n)$, we must show that there exists an element $\mathbf{N}\in\mathbf{U}$ such that $\mathbf{d}(\mathbf{M},\mathbf{N})$ is bounded as in (4.3). It is helpful here to consider $\mathbf{N}$ as being constructed by a sequence of "moves," starting from $\mathbf{M}$. The moves are defined by planar rotations, $\mathbf{T}_i$, for which $\mathbf{T}_1\mathbf{T}_2\ldots\mathbf{T}_{n-1} = \mathbf{N}\mathbf{M}^{-1}$. The transformations are unique provided that none of them have -1 as an eigenvalue, or, equivalently, that they do not rotate any vector by an angle of π radians.

First, let us consider the case of $\mathbf{SO}(3)$, as shown in Figure 4.1. Here, the transformation $\mathbf{N}\mathbf{M}^{-1}$ is reduced to a pair of planar rotations that have a nice characterization using the projective Euclidean metric. The transformation $\mathbf{T}_2$ maps the vector $\mathbf{u}_2$ to a nearby vector $\mathbf{w}_2\in\mathbf{U}^2$. Next, $\mathbf{T}_1$ maps $\mathbf{v}_1 = \mathbf{T}_2\mathbf{u}_1$ to a nearby vector $\mathbf{w}_1\in\mathbf{U}^1$. There is only one element, $\mathbf{N}\in\mathbf{SO}(3)$, for which $\mathbf{N}\mathbf{x}_1 = \mathbf{w}_1$ and $\mathbf{N}\mathbf{x}_2 = \mathbf{w}_2$. By construction, $\mathbf{N}$ is contained in our discrete sample, $\mathbf{U}\subset\mathbf{SO}(3)$, and we can show its distance to $\mathbf{M}\in\mathbf{SO}(3)$ is bounded as in (4.3).

More generally, given $\mathbf{u}_{n-1} = \mathbf{v}_{n-1}$, there exists $\mathbf{w}_{n-1} = \mathbf{N}\mathbf{x}_{n-1}\in\mathbf{U}^{n-1}$ for which

$$||\mathbf{v}_{n-1} - \mathbf{w}_{n-1}|| \le \boldsymbol{\rho}\cdot\frac{\mathbf{s}}{2}\sqrt{n-1}.$$

This follows from the properties of $\mathbf{U}^{n-1} = \mathbf{V}^{n-1}$. Now, define $\mathbf{T}_{n-1}$ to be the transformation that rotates $\mathbf{v}_{n-1}$ to $\mathbf{w}_{n-1}$ along a geodesic in $\mathbf{S}^{n-1}$. This transformation is unique unless $\mathbf{v}_{n-1} = -\mathbf{w}_{n-1}$, and we only require its existence. The next step is to define $\mathbf{v}_{n-2} = (\mathbf{T}_{n-1})\mathbf{u}_{n-2}$. Since there exists $\mathbf{w}_{n-2} = \mathbf{N}\mathbf{x}_{n-2}$ in $\mathbf{U}^{n-2}$ such that

$$||\mathbf{v}_{n-2} - \mathbf{w}_{n-2}|| \le \boldsymbol{\rho}\cdot\frac{\mathbf{s}}{2}\sqrt{n-2},$$

we define $\mathbf{T}_{n-2}$ as the transformation that fixes $\mathbf{w}_{n-1}$ and rotates $\mathbf{v}_{n-2}$ to $\mathbf{w}_{n-2}$. At each stage, a new transformation, $\mathbf{T}_i$, fixes the correctly mapped unit vectors,

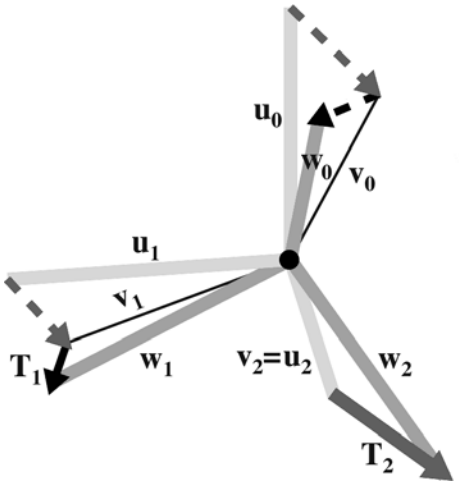

FIG. 4.1. *A Pythagorean theorem on* $\mathbf{SO}(n)$. *The proof of Theorem* 2 *is illustrated for the case* $n = 3$. *The orthonormal vectors* $\{\mathbf{u}_i = \mathbf{M}\mathbf{x}_i\}$, *shown in light gray, are rotated to the orthonormal vectors* $\{\mathbf{w}_i = \mathbf{N}\mathbf{x}_i\}$, *shown in medium gray, through intermediate vectors* $\{\mathbf{v}_i\}$, *shown using thin black lines. Given* $\mathbf{M}$, *a nearby rotation* $\mathbf{N}$ *is constructed using two planar rotations. The first such transformation,* $\mathbf{T}_2$, *maps* $\mathbf{v}_2 = \mathbf{u}_2$ *to* $\mathbf{w}_2$ *using a planar transformation, and the solid dark gray arrow represents the distance* $||\mathbf{v}_2 - \mathbf{w}_2||$. *The two dotted dark gray arrows indicate how* $\mathbf{T}_2$ *maps the vectors* $\mathbf{u}_0$ *and* $\mathbf{u}_1$. *The second, mapping between* $\mathbf{v}_1 = \mathbf{T}_2\mathbf{u}_1$ *and* $\mathbf{w}_1 = \mathbf{N}\mathbf{x}_1$, *is accomplished via a planar rotation,* $\mathbf{T}_1$, *as defined by the black arrows. The solid black arrow indicates the actual "cost" of the rotation,* $||\mathbf{v}_1 - \mathbf{w}_1||$. *The dotted black arrow indicates that* $\mathbf{v}_0 = \mathbf{T}_2\mathbf{u}_0$ *is mapped automatically to* $\mathbf{w}_0$ *by the construction, because the vectors* $\mathbf{v}_0, \mathbf{w}_0, \mathbf{v}_1$, *and* $\mathbf{w}_1$ *all lie in the plane orthogonal to* $\mathbf{w}_2$. *The distance* $\mathbf{d}(\mathbf{M}, \mathbf{N})$ *is bounded according to the lengths of the two solid arrows associated to the transformations* $\mathbf{T}_1$ *and* $\mathbf{T}_2$, *using a Pythagorean-like theorem for the metric* $\mathbf{d}$.

$\mathbf{w}_{i+1}, \ldots, \mathbf{w}_{n-1}$, and rotates an additional $\mathbf{v}_i$ to $\mathbf{w}_i$ within their mutual plane. This amounts to the following process, working recursively backward from $i = (n-1)$ to $i = 1$:

Define the vector $\mathbf{v}_i$:	$\mathbf{v}_i = (\mathbf{T}_{i+1} \cdots \mathbf{T}_{n-1})\,\mathbf{u}_i$;
Choose $\mathbf{w}_i \in \mathbf{U}^i$ to satisfy	$\|\|\mathbf{v}_i - \mathbf{w}_i\|\| \le \boldsymbol{\rho} \cdot \frac{\mathbf{s}}{2}\sqrt{i}$;
Choose a planar map $\mathbf{T}_i$ to satisfy	$\mathbf{T}_i\mathbf{v}_i = \mathbf{w}_i$.

The final vector $\mathbf{w}_0 = \mathbf{N}\mathbf{x}_0$ is uniquely defined as $\mathbf{w}_0 = (\mathbf{T}_1\mathbf{T}_2 \cdots \mathbf{T}_{n-1})\,\mathbf{u}_0$. Another way to think of this process is in terms of the following table of maps.

$$
\begin{array}{lllll}
\mathbf{u}_{n-1} & \overset{I}{\longrightarrow} & \mathbf{v}_{n-1} & \overset{T_{n-1}}{\longrightarrow} & \mathbf{w}_{n-1} \\
\mathbf{u}_{n-2} & \overset{T_{n-1}}{\longrightarrow} & \mathbf{v}_{n-2} & \overset{T_{n-2}}{\longrightarrow} & \mathbf{w}_{n-2} \\
\mathbf{u}_{n-3} & \overset{T_{n-2}T_{n-1}}{\longrightarrow} & \mathbf{v}_{n-3} & \overset{T_{n-3}}{\longrightarrow} & \mathbf{w}_{n-3} \\
 & & \cdots & & \\
\mathbf{u}_1 & \overset{T_2 \cdots T_{n-1}}{\longrightarrow} & \mathbf{v}_1 & \overset{T_1}{\longrightarrow} & \mathbf{w}_1 \\
\mathbf{u}_0 & \overset{T_1T_2 \cdots T_{n-1}}{\longrightarrow} & \mathbf{v}_0 & \overset{I}{\longrightarrow} & \mathbf{w}_0
\end{array}
$$

The maps to the right are operations we define. The maps to the left compose these transformations to define each $\mathbf{v}_i$, from which the next $\mathbf{w}_i$ and $\mathbf{T}_i$ are defined. Because

$\mathbf{T}_i$ fixes $\mathbf{w}_{i+1}, \ldots, \mathbf{w}_{n-1}$, it acts nontrivially on the first $(i+1) \times (i+1)$ subspace of $\mathbb{R}^n$, and it is the identity on the orthogonal $(n-i-1)$-dimensional subspace.

We have now constructed $\mathbf{NM}^{-1} \in \mathbf{SO}(n)$ using a sequence of planar rotations. The final goal is to bound $\mathbf{d}(\mathbf{M}, \mathbf{N})$ using the norms of the $\mathbf{T}_i$, which are the distances between the $\mathbf{v}_i$ and $\mathbf{w}_i$. Each $\mathbf{T}_i$ is defined by a single rotation angle, $\boldsymbol{\tau}_i$, in the plane containing vectors $\mathbf{v}_i$ and $\mathbf{w}_i$. The following three equalities are immediate:

$$\begin{aligned}
\mathbf{Tr}(\mathbf{I} - \mathbf{T}_i) &= 2\left(1 - \cos(\boldsymbol{\tau}_i)\right), \\
||\mathbf{v}_i - \mathbf{w}_i|| &= 2\sin\left(\frac{\boldsymbol{\tau}_i}{2}\right), \quad \text{and} \\
||\mathbf{I} - \mathbf{T}_i||^2 &= 2||\mathbf{v}_i - \mathbf{w}_i||^2.
\end{aligned}$$

The factor of two arises because the $\mathbf{T}_i$ are planar rotations and therefore rotate a pair of orthogonal eigenvectors by an angle of $\boldsymbol{\tau}_i$, or a distance of $||\mathbf{v}_i - \mathbf{w}_i||$.

The remaining steps involve noting that

$$\mathbf{d}^2(\mathbf{M}, \mathbf{N}) = \frac{1}{2}||\mathbf{I} - \mathbf{NM}^{-1}||^2$$

and considering the following telescoping sum:

$$\begin{aligned}
\mathbf{I} - \mathbf{NM}^{-1} &= \mathbf{I} - (\mathbf{T}_1\mathbf{T}_2\cdots\mathbf{T}_{n-1}) \\
&= [\mathbf{I} - \mathbf{T}_1] + [\mathbf{T}_1 - \mathbf{T}_1\mathbf{T}_2] + \cdots + [(\mathbf{T}_1\cdots\mathbf{T}_{n-2}) - (\mathbf{T}_1\cdots\mathbf{T}_{n-1})].
\end{aligned}$$

From the properties of the Froebenius norm, we get a Pythagorean-like theorem as follows:

$$\begin{aligned}
\mathbf{d}^2(\mathbf{M}, \mathbf{N}) &= \frac{1}{2}||\mathbf{I} - \mathbf{NM}^{-1}||^2 \\
&\leq \frac{1}{2}\left(||\mathbf{I} - \mathbf{T}_1||^2 + ||\mathbf{T}_1 - \mathbf{T}_1\mathbf{T}_2||^2 + \cdots + ||(\mathbf{T}_1\cdots\mathbf{T}_{n-2}) - (\mathbf{T}_1\cdots\mathbf{T}_{n-1})||^2\right) \\
&= \frac{1}{2}||\mathbf{I} - \mathbf{T}_1||^2 + \frac{1}{2}||\mathbf{I} - \mathbf{T}_2||^2 + \cdots + \frac{1}{2}||\mathbf{I} - \mathbf{T}_{n-1}||^2 \\
&= \sum_{i=1}^{n-1} \frac{1}{2}||\mathbf{I} - \mathbf{T}_i||^2 \\
&= \sum_{i=1}^{n-1} ||\mathbf{v}_i - \mathbf{w}_i||^2.
\end{aligned}$$

The reader should note that the sums in this section are distinct from the calculation of $\mathbf{d}^2$ as the sum of n terms involving squared distances between the $\mathbf{u}_i$ and $\mathbf{w}_i$. Here, we bound $\mathbf{d}^2$ using $(n-1)$ terms involving distances between the $\mathbf{v}_i$ and $\mathbf{w}_i$.

Now, by definition of the $\mathbf{w}_i$, the distances above are bounded as

$$||\mathbf{v}_i - \mathbf{w}_i|| \leq \boldsymbol{\rho} \cdot \frac{\mathbf{s}}{2} \cdot \sqrt{i},$$

where $\mathbf{s}$ is the target length step. Putting it all together, we have

$$\begin{aligned}\mathbf{d}^2(\mathbf{M},\mathbf{N}) &\le \sum_{i=1}^{n-1} \frac{1}{2}||\mathbf{I}-\mathbf{T}_i||^2 \\ &= \sum_{i=1}^{n-1} ||\mathbf{v}_i - \mathbf{w}_i||^2 \\ &\le \sum_{i=1}^{n-1} \left(\boldsymbol{\rho}\cdot\frac{\mathbf{s}}{2}\cdot\sqrt{i}\right)^2 \\ &= \left(\boldsymbol{\rho}\cdot\frac{\mathbf{s}}{2}\cdot\sqrt{m}\right)^2,\end{aligned}$$

and thus

$$\mathbf{d}(\mathbf{M},\mathbf{N}) \le \boldsymbol{\rho}\cdot\frac{\mathbf{s}}{2}\cdot\sqrt{m}.$$

We have shown that for any $\mathbf{M}\in\mathbf{SO}(n)$, there exists $\mathbf{N}\in\mathbf{U}$ for which (4.3) holds, and so $\mathbf{U}$ is a $\{\boldsymbol{\alpha},\boldsymbol{\rho}\}$-covered subset of $\mathbf{SO}(n)$. ∎

5. Conclusions. Here, we have presented the SOI algorithm for uniform deterministic sampling of rotation groups and demonstrated that it performs well with regard to many measures of sampling quality. The SOI method samples rotation space in a way that optimizes local separation and global coverage. The samples are well dispersed, and they have low energies relative to a range of repulsive orders.

We have shown a precise relationship between the global coverage and local separation properties of SOI samples, based on the coverage and separation properties of the spherical samples used to generate them. In the future, it may also be worth exploring the discrepancy of SOI samples. One anticipates that applying the SOI method using low-discrepancy $\mathbf{V}^i$ will result in a low-discrepancy sample on $\mathbf{SO}(n)$, but this has yet to be established.

In conjunction with this paper, codes and other resources for rotational sampling are available. At the time of this writing, they are most easily obtained via the author's website (http://mitchell-lab.org).

Appendix A. Parameterizations of SO(3).

A.1. Quaternion representation. Each unit quaternion, $\mathbf{q}=(q_1,q_2,q_3,q_4)$ and $||\mathbf{q}||=1$, defines an element of $\mathbf{SO}(3)$ according to the following formula:

$$\mathbf{M}_\mathbf{q} = \begin{bmatrix} q_1^2+q_2^2-q_3^2-q_4^2 & 2\cdot(q_2q_3-q_1q_4) & 2\cdot(q_2q_4+q_1q_3) \\ 2\cdot(q_2q_3+q_1q_4) & q_1^2-q_2^2+q_3^2-q_4^2 & 2\cdot(q_3q_4-q_1q_2) \\ 2\cdot(q_2q_4-q_1q_3) & 2\cdot(q_3q_4+q_1q_2) & q_1^2-q_2^2-q_3^2+q_4^2 \end{bmatrix}.$$

The unit quaternions arise from the isomorphism of the real projective space $\mathbb{RP}^3$ with $\mathbf{SO}(3)$. The angular distance between two unit quaternions is the same as the angular distance between the matrices defined by them. The space $\mathbf{S}^3$ parameterizes $\mathbb{RP}^3$ (and hence $\mathbf{SO}(3)$) as a locally isometric double cover. Thus, by sampling the unit quaternions uniformly, one can generate uniform samples on $\mathbf{SO}(3)$.

A.2. Axis-angle representation. The quaternion parameterization is related to the "axis-angle" representation. Given a unit vector $\mathbf{w}=(w_1,w_2,w_3)$ and rotation

angle $\boldsymbol{\alpha}$, the rotation matrix can be defined as

$$\mathbf{M}_{\mathbf{w},\boldsymbol{\alpha}} = \begin{bmatrix} 1+(w_1^2-1)\cdot(1-\cos\boldsymbol{\alpha}) & -w_3\cdot\sin\boldsymbol{\alpha}+w_1w_2\cdot(1-\cos\boldsymbol{\alpha}) & w_2\cdot\sin\boldsymbol{\alpha}+w_1w_3\cdot(1-\cos\boldsymbol{\alpha}) \\ w_3\cdot\sin\boldsymbol{\alpha}+w_1w_2\cdot(1-\cos\boldsymbol{\alpha}) & 1+(w_2^2-1)\cdot(1-\cos\boldsymbol{\alpha}) & -w_1\cdot\sin\boldsymbol{\alpha}+w_2w_3\cdot(1-\cos\boldsymbol{\alpha}) \\ -w_2\cdot\sin\boldsymbol{\alpha}+w_1w_3\cdot(1-\cos\boldsymbol{\alpha}) & w_1\cdot\sin\boldsymbol{\alpha}+w_2w_3\cdot(1-\cos\boldsymbol{\alpha}) & 1+(w_3^2-1)\cdot(1-\cos\boldsymbol{\alpha}) \end{bmatrix}.$$

The axis-angle representation is specific to $\mathbf{SO}(3)$, as its elements can be defined according to a single rotation angle. Elements of $\mathbf{SO}(n)$ can have multiple angles of rotation, each of which transforms a planar eigenspace.

This parameterization is not a local isometry. It is easy to make the mistake of sampling rotation space by choosing a random axis and random angle of rotation, and such mistakes have made it into press [1, 2]. This unintuitive fact is related to the fact that eigenvalues of rotation matrices are not uniformly distributed, and there are more large ($\geq \pi/2$) rotation angles than small ones [9].

A.3. Euler angle representation. An Euler angle triplet, $\boldsymbol{\Theta} = (\boldsymbol{\theta}_1, \boldsymbol{\theta}_2, \boldsymbol{\theta}_3)$, parameterizes any rotation as the composition of three planar rotations about canonical axes. There are numerous conventions for using Euler angles to construct elements of $\mathbf{SO}(3)$. Each is useful, but all have an equivalent problem. The identity matrix can be described by infinitely many Euler angle triplets. The practical impact is that two Euler angles can appear very different, yet map to rotation matrices that are nearby in $\mathbf{SO}(3)$. There is a singular metric distortion that actually changes the topology of the parameter space in comparison with the parameterized space.

Euler angles do, however, have some practical applications and remain a useful construct. Here is one possible convention for specifying a rotation matrix using a pair of angles $\boldsymbol{\theta}_1, \boldsymbol{\theta}_3 \in [-\pi, \pi]$ and $\boldsymbol{\theta}_2 \in [0, \pi]$, and there are many others found in the engineering and science literature. Defining $c_i = \cos\boldsymbol{\theta}_i$ and $s_i = \sin\boldsymbol{\theta}_i$, a rotation matrix can be defined as

$$\mathbf{M}_{\boldsymbol{\Theta}} = \begin{bmatrix} c_1\cdot c_3 - s_1\cdot c_2\cdot s_3 & -c_1\cdot s_3 - s_1\cdot c_2\cdot c_3 & s_1\cdot s_2 \\ s_1\cdot c_3 + c_1\cdot c_2\cdot s_3 & -s_1\cdot s_3 + c_1\cdot c_2\cdot c_3 & -c_1\cdot s_2 \\ s_2\cdot s_3 & s_2\cdot c_3 & c_2 \end{bmatrix}.$$

Sampling Euler angle space uniformly (in the Euler angles) is tantamount to sampling the sphere according to latitude and longitude. There are singularities at the poles, and the sampling density will be nonuniform there. If one considers the possible images of just the $\mathbf{x}_2$ axis, which are determined by the angles $\boldsymbol{\theta}_1$ and $\boldsymbol{\theta}_2$ according to the third column of $\mathbf{M}_{\boldsymbol{\Theta}}$, it is easy to see that they fail to be uniformly distributed over the surface of $\mathbf{S}^2$.

Acknowledgments. The following people are to be thanked for their suggestions and discussions of their related work: Bruce Donald, Rex Kerr, Steve LaValle, Michael Pique, Joel Robbin, Jean-Pierre Rosay, Peter Sarnak, Stephen Smale, Lynn Ten Eyck, Laura Vanderploeg, Alan Weinstein, Zhiping Weng, Shoshana Wodak, and Anna Yershova. The author also thanks the SIAM Journal on Scientific Computing editors and reviewers for their guidance.

REFERENCES

[1] J. Arvo, *Random Rotation Matrices*, Academic Press, Boston, 1991, pp. 355–356.
[2] J. Arvo, *Fast Random Rotation Matrices*, Academic Press, Boston, 1992, pp. 117–120.
[3] F. Aurenhammer and H. Edelsbrunner, *An optimal algorithm for constructing the weighted Voronoi diagram in the plane*, Pattern Recognition, 17 (1984), pp. 251–257.

[4] A. Barenco, C. H. Bennett, R. Cleve, D. P. Divincenzo, N. Margolus, P. Shor, T. Sleator, J. A. Smolin, and H. Weinfurter, *Elementary gates for quantum computation*, Phys. Rev. A, 52 (1995), pp. 3457–3467.
[5] A. Bjorck and G. H. Golub, *Numerical methods for computing angles between linear subspaces*, Math. Comp., 27 (1973), pp. 579–594.
[6] V. Bulatov, *Point Repulsion/Sphere Tesselation Code Available*, http://www.math.niu.edu/~rusin/known-math/96/repulsion (11 February 1996).
[7] R. Chen and Z. Weng, *Docking unbound proteins using shape complementarity, desolvation, and electrostatics*, Prot. Struct. Fun. Gen., 47 (2002), pp. 281–294.
[8] R. A. Crowther, *The fast rotation function in the molecular replacement method*, Int. Sci. Rev. Ser., 12 (1972), pp. 173–178.
[9] P. Diaconis, *Patterns in eigenvalues*, Bull. Amer. Math. Soc. (N.S.), 40 (2003), pp. 155–178.
[10] P. Diaconis and M. Shahshahani, *The subgroup algorithm for generating uniform random variables*, Probab. Eng. Inf. Sci., 1 (1987), pp. 15–32.
[11] G. L. Dirichlet, *Über die Reduktion der positiven quadratischen Formen mit drei unbestimmten ganzen Zahlen*, J. Reine Angew. Math., 40 (1850), pp. 209–227.
[12] B. R. Donald, *A search algorithm for motion planning with six degrees of freedom*, Artif. Intell., 31 (1987), pp. 295–353.
[13] R. Fisher, *Dispersion on a sphere*, Proc. Roy. Soc. London Ser. A, 217 (1953), pp. 295–305.
[14] W. M. Gentleman, *Least squares computations by Givens transformations without square roots*, IMA J. Appl. Math, 12 (1973), pp. 329–336.
[15] G. Golub and W. Kahan, *Calculating the singular values and pseudo-inverse of a matrix*, SIAM J. Numer. Anal., 2 (1965), pp. 205–224.
[16] D. P. Hardin and E. B. Saff, *Discretizing manifolds via minimum energy points*, Notices Amer. Math. Soc., 51 (2004), pp. 1186–1194.
[17] C. J. Langmead, A. K. Yan, L. Wang, R. Lilien, and B. Donald, *A polynomial time nuclear vector replacement algorithm for automated NMR resonance assignments*, J. Comp. Biol., 11 (2004), pp. 277–298.
[18] A. Lubotsky, R. Phillips, and P. Sarnak, *Hecke operators and distributing points on the sphere* I, Comm. Pure Appl. Math., 39 (1986), pp. S149–S138.
[19] J. G. Mandell, V. A. Roberts, M. E. Pique, V. Kotlovyi, J. C. Mitchell, E. Nelson, I. Tsigelny, and L. F. Ten Eyck, *Protein docking using continuum electrostatics and geometric fit*, Protein Eng., 14 (2001), pp. 105–113.
[20] J. Matousek, *Geometric Discrepancy*, Springer-Verlag, Berlin, 1999.
[21] J. Navaza, *On the fast rotation function*, Acta Cryst., A43 (1987), pp. 645–653.
[22] H. Niederreiter, *Random Number Generation and Quasi-Monte Carlo Methods*, CBMS-NSF Regional Conf. Ser. in Appl. Math. 63, SIAM, Philadelphia, 1992.
[23] J. A. Northby, *Structure and binding of Lennard–Jones clusters:* $13 \leq n \leq 147$, J. Chem. Phys., 87 (1987), pp. 6166–6177.
[24] E. B. Saff and A. B. J. Kuijlaars, *Distributing many points on a sphere*, Math. Intelligencer, 19 (1997), pp. 5–14.
[25] N. J. A. Sloane, T. S. D. R. H. Hardin, and J. H. Conway, *Minimal-energy clusters of hard spheres*, Discrete Comput. Geom., 14 (1995), pp. 237–259.
[26] S. Smale, *Mathematical problems for the next century*, Math. Intelligencer, 20 (1998), pp. 7–15.
[27] G. W. Stewart, *The efficient generation of random orthogonal matrices with an application to condition estimators*, SIAM J. Numer. Anal., 17 (1980), p. 403–409.
[28] G. Voronoi, *Nouvelles applications des parametres continus e la theorie des formes quadratiques*, J. Reine Angew. Math., 133 (1907), pp. 97–178.
[29] D. Wales and J. Doye, *Global optimization by basin-hopping and the lowest energy structures of Lennard–Jones clusters containing up to* 110 *atoms*, J. Phys. Chem. A, 101 (1997), pp. 5111–5116.
[30] H. Weyl, *Über die Gleichverteilung von Zahlen mod. Eins*, Math. Ann., 77 (1916), pp. 313–352.
[31] S. J. Wodak and J. Janin, *Computer analysis of protein-protein interaction*, J. Mol. Biol., 124 (1978), pp. 323–342.
[32] A. Yan, C. Langmead, and B. R. Donald, *A probability-based similarity measure for Saupe alignment tensors with applications to residual dipolar couplings in NMR structural biology*, Int. J. Robotics Res., 24 (2005), pp. 165–182.
[33] A. Yershova and S. LaValle, *Deterministic sampling methods for spheres and* $SO(3)$, in Proceedings of the IEEE International Conference on Robotics and Automation, Vol. 4, 2004, pp. 3974–3980.
[34] K. Zyczkowski and M. Kus, *Random unitary matrices*, J. Phys. A, 27 (1994), pp. 4235–4245.